

Functional renormalization of QCD in 1 + 1 dimensions: four-fermion interactions from quark-gluon dynamics

Eric Oevermann ^{1,*} Adrian Koenigstein ^{1,†} and Stefan Floerchinger ^{1,‡}

¹*Institute for Theoretical Physics, Schiller University, Max-Wien-Platz 1, 07743 Jena, Germany*

(Dated: December 23, 2024)

Quantum Chromodynamics in two spacetime dimensions is investigated with the Functional Renormalization Group. We use a functional formulation with covariant gauge fixing and derive Renormalization Group flow equations for the gauge coupling, quark mass and an algebraically complete set of local fermion-fermion interaction vertices. The flow, based on a convenient Callan–Symanzik-type regularization, shows the expected behavior for a super-renormalizable theory in the ultraviolet regime and leads to a strongly coupled regime in the infrared. Through a detailed discussion of symmetry implications, and variations in the gauge group and flavor numbers, the analysis sets the stage for a more detailed investigation of the bound state spectrum in future work.

Keywords: two-dimensional QCD, 't Hooft model, Functional Renormalization Group, four-fermion interactions, Fierz completeness

CONTENTS

		F. Contribution to quark two-point vertex	21
I. Introduction	1	VII. Outlook: bosonization	22
A. Contextualisation	2	VIII. Summary and conclusion	22
B. Research objective	2	Acknowledgements	23
C. Structure	2	A. BRST symmetry	23
D. Supplementary material	3	B. Ward identity for CS-type regulators	23
II. The model	3	C. Derivation of the modified Nielsen identity	24
A. The microscopic theory	3	D. Rescaling of the gauge field	25
B. Symmetries	3	E. Infinite- N_c limit of four-fermion flow equations	25
III. Quantum effective action	4	References	26
A. Gauge fixing, background-field method and the quantum effective action	4		
B. Gauge invariance and BRST symmetry	5		
C. Ward identities	6		
D. Regularization via a local regulator	6		
IV. The method: the FRG	7		
V. Quantum effective action: minimal ansatz	7		
A. A minimal truncation	8		
B. Running quark mass and wave function	8		
C. Running gauge coupling	9		
D. Consistency check: the quark-gluon vertex	10		
E. Limiting cases	10		
F. Summary of the chapter	14		
VI. (Local) four-fermion interactions	14		
A. Extended truncation	14		
B. Connection to other four-fermion models	15		
C. Deriving flow equations	16		
D. Limiting cases	17		
E. Regulator dependences	21		

I. INTRODUCTION

The study of nonperturbative phenomena in Quantum Field Theory (QFT) is challenging but crucial for understanding many intriguing properties of strongly interacting systems in solid state and high-energy physics. A prime example is the theory of Quantum Chromodynamics (QCD) exhibiting confinement, chiral symmetry breaking, hadron formation, multiple thermodynamic phases, *etc.* which are all not fully understood yet [1]. One out of many approaches to make progress on these questions is to investigate lower-dimensional models since they are often more tractable and even admit exact solutions [2]. Usually one can study particular aspects of a theory in this simplified setting and then try to transfer the insights to the more complex case in higher dimensions.

* eric.oevermann@uni-jena.de

† adrian.koenigstein@uni-jena.de

‡ stefan.floerchinger@uni-jena.de

A. Contextualisation

In this work, we inspect two-dimensional Quantum Chromodynamics (QCD₂) which is naturally related to QCD. Here, one can address many of the questions of interest for QCD but in a simpler setting. The theory becomes super-renormalizable and possesses much fewer degrees of freedom than in four dimensions, but keeps most of the other important properties of QCD, like confinement. Yet, it serves as a more realistic toy model for QCD than, *e.g.*, the Schwinger model that also shows confinement because of its geometric origin in two dimensions where the Coulomb potential between static (color) charges rises linearly with their distance [3].

QCD₂ has been studied in various contexts and for a plenty of reasons. In Fig. 1, we tried to sketch some connections and highlight some motivations. For detailed reviews we refer to Refs. [2, 3]. Here, we shall only list some of the most important aspects of the model: The

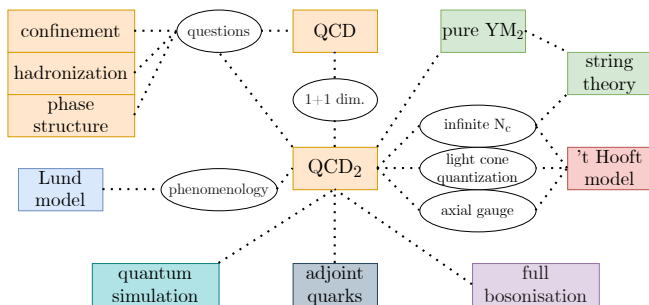


FIG. 1. Overview of various interests in the literature in studying QCD₂.

restriction to two dimensions is phenomenologically motivated by the Lund (string) model for the dynamics of hadronization [4]. Besides, QCD₂ has been solved analytically in the limit of an infinite number of colors, $N_c \rightarrow \infty$, and at one flavor which is referred to as the 't Hooft model [5]. With QCD, it shares the properties of confinement, asymptotic freedom, chiral symmetry breaking [6] and the existence of a rich bound state spectrum of mesons. Baryons emerge in the next-to-leading order in a $1/N_c$ -expansion [7] for which QCD₂ was the first application and test, see also Ref. [8]. In addition, the 't Hooft model presents an important toy model exploring light-cone quantization [9, 10]. Much progress has been made on the integrability of the model in this particular limit that is also still an active field of research [11–13] and even thermodynamic properties have been explored [2, 14]. Moreover, this limit establishes a connection to string theory if one concentrates on pure gauge theory [3, 15, 16]. Interestingly, two-dimensional Yang–Mills (YM₂) is even soluble at finite N_c [17–19].

We are interested in the model at a finite number of colors and flavors bridging between the 't Hooft model and QCD. This case has been studied with (non-Abelian) full bosonization techniques in analogy to approaches

to the Schwinger model, see Refs. [3, 20] for reviews and Refs. [21, 22] for recent applications. Furthermore, quarks in the adjoint representation of the $SU(N_c)$ gauge group have been considered [3] for which the model behaves very differently in the infrared (IR) becoming deconfining, see, *e.g.*, Refs. [23, 24] for latest studies. Recently, even quantum simulations of QCD₂ are subject of discussion [25–29].

B. Research objective

We take QCD₂ at finite number of colors and flavors as an exemplary model for investigating the dynamical emergence of bound states. Therefore, our medium-term goal is the systematic application and improvement of dynamical partial bosonization techniques using Functional Renormalization Group (FRG) methods. There are already several QCD related works in four dimensions reaching from Fierz-complete truncations to full effective mesonic potentials to which we refer in Section VI. In the future, we wish to utilize the simplifications that arise in two dimensions to resolve the for this purpose crucial four-fermion interactions in more detail than it is currently feasible in four dimensions.

This work presents the first FRG study of QCD₂ and we establish the very first steps towards this goal. In particular, we demonstrate that simple Callan–Symanzik-type regulators are usable in two dimensions which also motivates our approach since they preserve important symmetries and analyticities. We concentrate on the case of zero temperature and quark chemical potentials but consider limits of infinite number of colors or flavors too, because a re-derivation of the 't Hooft solution with the FRG and a connection to other models is a further goal.

The intermediate achievements of our program that we discuss in this work comprise the study of the minimal ansatz for the effective average action in the gluonic sector and the additional inclusion of a set of Fierz-complete, local four-fermion interactions that are generated from the gauge dynamics. This already allows to identify relevant channels for bosonization as well as robust understanding of the dynamics in the ultraviolet (UV) as well as in different limiting cases.

C. Structure

This work is structured as follows: we first review the microscopic QCD₂-action and its symmetries in Section II. Since we deal with a gauge theory, we next survey the steps towards the computation of its quantum effective action in Section III. This includes the introduction of the background-field method and a discussion of a regularization of Callan–Symanzik type for the fluctuating part of the gauge field. Besides, we briefly explain the FRG approach and the use of Callan–Symanzik-type regulators in Section IV. We are then ready for

an initial investigation of the model close to perturbation theory in Section V. In Section VI, we include a set of Fierz-complete, local four-fermion interactions in the ansatz for the effective average action. This section can partly be seen as a standalone Fierz-complete study of a purely fermionic theory in two dimensions. Bosonization of these interactions is mentioned in the Outlook, Section VII. We conclude in Section VIII. More details on certain aspects of the discussion in the main text are provided in the appendix.

D. Supplementary material

Instead of providing all (lengthy) calculations in the main text or adding further detailed appendices, we decided to refer to the (online available) Master's thesis of Eric Oevermann [30] for technical details and conventions. This should make the paper more readable, avoid redundancy, and on the other hand assures that all calculations are available to the reader for the sake of transparency and reproducibility. Conventions are the same.

II. THE MODEL

In this section, we introduce the theory under investigation on a formal level.

A. The microscopic theory

The microscopic action for QCD₂ in Euclidean spacetime is

$$S_{\text{QCD}_2}[A, \bar{\psi}, \psi] = \int_x \mathcal{L}(x) \quad (1)$$

with the Lagrangian

$$\mathcal{L} = \bar{\psi} (\gamma^\mu D_\mu + m) \psi + \frac{1}{2g^2} \text{tr}(F_{\mu\nu} F^{\mu\nu}). \quad (2)$$

The domain of integration is \mathbb{R}^2 at zero temperature. The relation to the action in Minkowski spacetime is discussed in detail, *e.g.*, in Ref. [30, Sec. 2 and App. A]. Fermions ψ and anti-fermions $\bar{\psi}$, which we also call quarks and anti-quarks, carry color charge in the fundamental representation of the gauge group and come in N_f flavors. Hence, in index notation they have a color index, $c \in \{1, \dots, N_c\}$, a flavor index $f \in \{1, \dots, N_f\}$, and a Dirac index $a \in \{1, \dots, d_\gamma\}$, which we selectively suppress in equations.

The fermions are supposed to have a bare mass m which is here approximated to be identical for all flavors. The quarks are coupled to the gauge field A via

the gauge-covariant derivative with matrix-valued gauge fields,

$$D_\mu = \partial_\mu - iA_\mu, \quad A_\mu = A_\mu^z T_z. \quad (3)$$

The matrices T_z with $z \in \{1, \dots, N_c^2 - 1\}$ are the hermitian generators of the $SU(N_c)$ gauge group (in the fundamental representation) and obey the commutation relation

$$[T_z, T_w] = i f_{zw}^v T_v, \quad (4)$$

where f_{zw}^v are the structure constants of the Lie algebra. We use the orthogonality relation and normalization

$$\text{tr}(T_w T_z) = C(r) \delta_{wz}, \quad (5)$$

where

$$C(r) = \begin{cases} 1/2, & \text{fundamental representation,} \\ N_c, & \text{adjoint representation.} \end{cases} \quad (6)$$

In addition, g is the gauge coupling and the components of the field-strength tensor are

$$F_{\mu\nu} = \partial_\mu A_\nu - \partial_\nu A_\mu - i[A_\mu, A_\nu]. \quad (7)$$

A peculiarity in two dimensions is that the gauge field has no propagating degrees of freedom, which follows from gauge freedom and the equations of motion. In the perturbative limit, instead of propagating gluons one has just a Coulomb-like interaction that is mediated by the field A_μ . In two dimensions, it gives rise to a linear potential between colored charges [31, 32], see Ref. [33] for a detailed discussion. Already this geometric property leads to an expectation to find color confinement. In this sense, we expect signals of color confinement in our results.

Before we continue, let us briefly comment on the scaling dimensions of the fields in a two-dimensional spacetime. In general, fields have energy dimensions

$$[\psi] = E^{\frac{d-1}{2}} \stackrel{d=2}{=} E^{\frac{1}{2}}, \quad [A] = E. \quad (8)$$

Consequently, one finds

$$[g] = E^{\frac{4-d}{2}} \stackrel{d=2}{=} E \quad (9)$$

for the gauge coupling. The fact that the gauge coupling has positive energy dimension makes the theory superrenormalizable in the perturbative domain.

B. Symmetries

The model possesses several symmetries in vacuum [31]. It is constructed to be gauge invariant, where the fermions are supposed to transform under the fundamental representations of the gauge group $SU(N_c)$. In addition, in Minkowski space, fermions transform as two-dimensional spinors under Lorentz transformations while

the gauge field is one form. In Euclidean spacetime, the Lorentz group $SO(1,1)$ turns into the rotation group $SO(2)$ and the corresponding algebra for the Euclidean gamma matrices is

$$\{\gamma^\mu, \gamma^\nu\} = 2 \mathbb{1} \delta^{\mu\nu}. \quad (10)$$

We again refer to Ref. [30, Sec. 2 and App. A & B] for details on our conventions for the Dirac matrices and on spacetime symmetries in Minkowski and Euclidean space. In short, the action is invariant under the continuous proper orthochronous Lorentz transformations as well as the discrete operations of parity, time reversal, and charge conjugation and their respective Euclidean analogues. In addition, the extension to the group of Poincaré transformations is a symmetry.

The fermions also constitute a fundamental representation of the flavor group. If there was no mass term, the action would be invariant under $U_L(N_f) \times U_R(N_f)$, independent global flavor rotations for the left- and right-handed components. The symmetry reduces to $U(N_f) \cong SU(N_f) \times U(1)/\mathbb{Z}_{N_f}$ for non-zero quark masses. Invariance under global phase rotations $U(1)$ corresponds to baryon number conservation. Axial transformations $U_A(1)$ are no symmetry in presence of the fermion mass, but it is interesting to note that QCD is anomaly-free in two dimensions [32], see also Ref. [30, App. D]. Hence, a massless one-flavor theory would remain massless (in a perturbative setup) and the presence of chiral symmetry would set important restrictions on possible fermion interactions being generated via quantum fluctuations.

In any case, the Coleman–Mermin–Wagner–Hohenberg–Berezinskii theorem [34–38] implies that we cannot expect spontaneous symmetry breaking of a continuous global symmetry in our model at finite N_c and finite N_f . The physical contradiction, if this was possible, would be a growing correlation function of the appearing Goldstone bosons with increasing distances [32]. There is still the possibility of a Berezinskii–Kosterlitz–Thouless phase-transition [37–39] at vanishing temperature $T = 0$ which is not associated with spontaneous symmetry breaking but with a divergence of the correlation length.

We conclude the symmetry discussion by pointing out that there is no dilatation or conformal symmetry, even for massless quarks, as it can be seen from the positive energy dimension of the gauge coupling [31]. This is another significant difference to the microscopic theory of QCD in $3 + 1$ spacetime dimensions.

III. QUANTUM EFFECTIVE ACTION

We now want to formulate a quantum-field-theoretic description for QCD_2 by defining its partition function Z and its *quantum* or *one-particle irreducible effective action* Γ . The main goal of this section is to introduce the known background-field method in some detail such that the advantages of our scheme for regularizing the theory become comprehensible.

A. Gauge fixing, background-field method and the quantum effective action

Starting from the microscopic action (1), the first attempt to define the partition function Z in presence of sources is to simply integrate over all field configurations,

$$Z[\bar{\eta}, \eta, J] = \int \mathcal{D}\bar{\psi} \mathcal{D}\psi \mathcal{D}A \exp \left(- S_{\text{QCD}_2}[\bar{\psi}, \psi, A] + \int_x (\bar{\psi} \eta + \bar{\eta} \psi + J_z^\mu A_\mu^z) \right). \quad (11)$$

We face two challenges:

1. The path integral takes into account too many field configurations, since some are related by gauge transformations. Consequently, $S_{\text{QCD}_2}^{(2),AA}$, the bare “inverse” propagator, is in fact not invertible.
2. Moreover, we must regularize the theory, in particular the IR, as we will see.

Let us first turn our attention to the first point. We impose a gauge fixing condition,

$$G[A] \stackrel{!}{=} 0 \quad (12)$$

upon the gauge field A such that in the partition function,

$$Z[\bar{\eta}, \eta, J] = \int \mathcal{D}\bar{\psi} \mathcal{D}\psi \mathcal{D}A \delta(G[A]) \text{Det} \left(\frac{\delta}{\delta\alpha} G[A] \right) \times \exp \left(- S_{\text{QCD}_2}[\bar{\psi}, \psi, A] + \int_x (\bar{\psi} \eta + \bar{\eta} \psi + J_z^\mu A_\mu^z) \right), \quad (13)$$

only one representative of each gauge orbit is picked and we dropped the integral over the gauge orbits. The term $\delta G[A]/\delta\alpha$ denotes the variation with respect to (w.r.t.) the parameter α of an infinitesimal gauge transformation.

In a next step, we want to move on to the quantum effective action Γ . Hereby, we employ the background-field method to construct a manifestly gauge invariant Γ even though a gauge-fixing procedure has been applied [40–51]. To begin with, we shift the variable in the path integral

$$A = \bar{A} + a, \quad (14)$$

where \bar{A} is a background-field and a , being the fluctuation-field, is the new integration variable,

$$Z[\bar{\eta}, \eta, J, \bar{A}] = \int \mathcal{D}\bar{\psi} \mathcal{D}\psi \mathcal{D}a \delta(G[\bar{A}, a]) \times \text{Det} \left(\frac{\delta}{\delta\alpha} G[\bar{A}, a] \right) \exp \left(- S_{\text{QCD}_2}[\bar{\psi}, \psi, \bar{A} + a] + \int_x [\bar{\psi} \eta + \bar{\eta} \psi + J_z^\mu (\bar{A}_\mu^z + a_\mu^z)] \right). \quad (15)$$

Note that the source couples to the full field $A = \bar{A} + a$. In fact, it is equivalent to couple the sources to the

background field or to the fluctuation field only, to arrive at the gauge-invariant quantum effective action, see Ref. [50, Sec. 3].

We now impose the specific gauge fixing condition

$$0 \stackrel{\dagger}{=} G[a, \bar{A}]^z = (D^\mu[\bar{A}] a_\mu)^z - \sigma^z, \quad (16)$$

where σ^z is an arbitrary function of the spacetime coordinates. We integrate over all σ^z with a Gaussian weighting around $\sigma^z = 0$ [52, Secs. 9.4 & 16.2], and include the delta-distribution in the action as the term

$$S_{\text{gf}}[\bar{A}, a] = \frac{1}{\xi} \frac{1}{2g^2} \int_x (D_\mu[\bar{A}]^z{}_y a^{\mu y}) (D_\nu[\bar{A}]_{zx} a^{\nu x}). \quad (17)$$

The constant ξ can be chosen arbitrarily. Specifically, the choice $\xi = 1$ corresponds to the background-field analogue of Feynman–'t Hooft gauge [52, Sec. 16.6], while $\xi = 0$ is called the Landau–DeWitt gauge [53].

Furthermore, we express the determinant with the Faddeev–Popov procedure [54]. This leads to the introduction of the ghost fields c and \bar{c} [52, Secs. 16.2 & 16.6],

$$S_{\text{gh}}[a, \bar{A}, \bar{c}, c] = - \int_x \bar{c}_z D^\mu[\bar{A}]^z{}_w D_\mu[a + \bar{A}]^w{}_v c^v. \quad (18)$$

This method does not come without problems such as the famous Gribov copies [55, 56], see also Ref. [57] for a discussion of Gribov copies in two-dimensional gauge theories. Since we will not access the far IR regime of the theory in this paper, these problems are, for the time being, not very relevant to us. The total action now reads

$$S[\bar{\psi}, \psi, a, \bar{A}, \bar{c}, c] \quad (19)$$

$$= S_{\text{QCD}_2}[\bar{\psi}, \psi, \bar{A} + a] + S_{\text{gf}}[a, \bar{A}] + S_{\text{gh}}[a + \bar{A}, \bar{A}, \bar{c}, c],$$

and the partition function is given by

$$\begin{aligned} Z[\bar{\eta}, \eta, J, \bar{A}, \bar{\omega}, \omega] &= \quad (20) \\ &= \int \mathcal{D}\bar{\psi} \mathcal{D}\psi \mathcal{D}a \mathcal{D}c \mathcal{D}\bar{c} \exp \left(- S[\bar{\psi}, \psi, a, \bar{A}, \bar{c}, c] + \right. \\ &\quad \left. + \int_x [\bar{\psi} \eta + \bar{\eta} \psi + J_z^\mu (\bar{A}_\mu^z + a_\mu^z) + \bar{c} \omega + \bar{\omega} c] \right). \end{aligned}$$

The first step towards the construction of the quantum effective action is to define the Schwinger functional

$$W[\bar{\eta}, \eta, J, \bar{A}, \bar{\omega}, \omega] = \ln Z[\bar{\eta}, \eta, J, \bar{A}, \bar{\omega}, \omega]. \quad (21)$$

The quantum effective action Γ is defined as the Legendre transform of W ,

$$\Gamma[\bar{\psi}, \psi, a, \bar{A}, \bar{c}, c] \quad (22)$$

$$= \sup_{\bar{\eta}, \eta, J, \omega, \bar{\omega}} \left(\int_x [\bar{\psi} \eta + \bar{\eta} \psi + J_z^\mu (\bar{A}_\mu^z + a_\mu^z) + \bar{c} \omega + \bar{\omega} c] + \right.$$

$$\left. - W[\bar{\eta}, \eta, J, \bar{A}, \bar{\omega}, \omega] \right).$$

We identify the background-field \bar{A} with the expectation value of the gauge field A , denoted by A again, after all calculations. Not introducing a new variable for this quantum effective action we write

$$\Gamma[\bar{\psi}, \psi, A, \bar{c}, c] \equiv \Gamma[\bar{\psi}, \psi, a, \bar{A}, \bar{c}, c]|_{\bar{A}=A, a=0}. \quad (23)$$

B. Gauge invariance and BRST symmetry

We now discuss in what sense the background-field method ensures gauge invariance of the quantum effective action. The action S_{QCD_2} is invariant under a gauge transformation of the full field A which can be distributed in two ways over the fields a and \bar{A} . There is the *fluctuation-field gauge transformation* acting on the fluctuation-field a only,

$$\bar{A}_\mu^z \mapsto \bar{A}'_\mu{}^z = \bar{A}_\mu^z, \quad (24)$$

$$a_\mu^z \mapsto a'^\mu{}^z = a_\mu^z + D_\mu[a + \bar{A}]^z{}_y \alpha^y. \quad (25)$$

Alternatively, in the *background-field gauge transformation* the background-field transforms like a gauge field and the fluctuation-field as a matter field in the adjoint representation,

$$\bar{A}_\mu^z \mapsto \bar{A}'_\mu{}^z = \bar{A}_\mu^z + D_\mu[\bar{A}]^z{}_y \alpha^y, \quad (26)$$

$$a_\mu^z \mapsto a'^\mu{}^z = a_\mu^z + i\alpha^y (T_y^{(\text{adj})})^z{}_w a_\mu^w. \quad (27)$$

Note that the ghost fields also transform as matter fields in the adjoint representation under background-field transformations. The gauge-fixed action S is not invariant under the fluctuation-field gauge transformations Eqs. (24) and (25). However, it is invariant under the background-field gauge transformations Eqs. (26) and (27). As a consequence, the quantum effective action $\Gamma[\bar{\psi}, \psi, a, \bar{A}, \bar{c}, c]$ is also invariant under the background-field gauge transformations.

Finally, the quantum effective action $\Gamma[\bar{\psi}, \psi, A, \bar{c}, c]$ inherits gauge invariance under a gauge transformation of the full field A from the background-field gauge invariance, *c.f.* Refs. [50], [53, Sec. 5.2.1], [58, Sec. 2], [59, Sec. 4.1]. It is shown in Ref. [50, Sec. 3] that gauge invariance obtained in this way from the background-field method is equivalent to physical gauge invariance of the full field A derived without the background-field method. In other words, the equivalence follows from the background-independence of the approach (encoded in Nielsen identities) and Slavnov–Taylor identities [53, Sec. 5.2.1], which we discuss in the following.

There is also a residual symmetry of the gauge-fixed action S in Eq. (19), the Becchi–Rouet–Stora–Tyutin

(BRST) symmetry [60, 61], for which we provide details in Appendix A.

C. Ward identities

We now discuss a few identities which constrain the quantum effective action via the symmetries of the microscopic theory. To start with, before evaluating the quantum effective action $\Gamma[\bar{\psi}, \psi, a, \bar{A}, \bar{c}, c]$ at $\bar{A} = A$, $a = 0$, it has to satisfy the *Ward–Takahashi identity*

$$\mathcal{G}^z \Gamma[a, \bar{A}] = \langle \mathcal{G}^z (S_{\text{gf}} + S_{\text{gh}}) \rangle_{J[\Phi]}. \quad (28)$$

Here, \mathcal{G}^z is the generator of the fluctuation field gauge transformations whose explicit form is

$$\begin{aligned} \mathcal{G}^z = & D_\mu [a + \bar{A}]^z_w \frac{\delta}{\delta a_{\mu w}} + i (T^z \psi)^a \frac{\delta}{\delta \psi^a} \\ & - i (\bar{\psi} T^z)_a \frac{\delta}{\delta \bar{\psi}_a} + f^z_w{}^v c^w \frac{\delta}{\delta c^v} - f^z_{wv} \bar{c}^w \frac{\delta}{\delta \bar{c}_v}. \end{aligned} \quad (29)$$

The expression on the right hand side (r.h.s.) is evaluated at sources J that are functionals of the field expectation values. The identity encodes how $\Gamma[a, \bar{A}]$ transforms due to the invariance of the microscopic action S_{QCD_2} under fluctuation-field gauge transformations [59, Eqs. (49) and (83), Sec. 4.1]. These transformations are discussed in Ref. [58] in more detail.

Similarly, the BRST symmetry of the gauge-fixed action S leads to the *Slavnov–Taylor identity* for the quantum effective action [53, Sec. 5.2.1],

$$\mathcal{G} \Gamma = 0, \quad (30)$$

where \mathcal{G} generates the BRST transformations,

$$\begin{aligned} \mathcal{G} = & (D_\mu [a + \bar{A}]^z c)^z \frac{\delta}{\delta a_{\mu}^z} + i c^z (T_z \psi)^a \frac{\delta}{\delta \psi^a} \\ & - i c^z (\bar{\psi} T_z)_a \frac{\delta}{\delta \bar{\psi}_a} - \frac{1}{2} f^z_{uv} c^u c^v \frac{\delta}{\delta c^z} + B_z \frac{\delta}{\delta \bar{c}_z}. \end{aligned} \quad (31)$$

The background-independence of the background-field method is encoded in the *Nielsen identity* [53, Sec. 5.2.1],

$$\frac{\delta \Gamma[a, \bar{A}]}{\delta \bar{A}} = 0, \quad (32)$$

which is evaluated on-shell, *i.e.* at vanishing sources where $\delta \Gamma[a, \bar{A}]/\delta a = 0$.

D. Regularization via a local regulator

We have not yet discussed the regularization of the theory. The need for a UV-regularization is not anticipated since the theory is super-renormalizable. However,

severe IR-divergencies due to massless gauge fields are expected to occur in two dimensions.

Even though the following construction points towards the FRG approach, it only is meant to be a general regularization scheme at this stage. To this end, a regulator piece ΔS_k is added to the action S . We specify ΔS_k to be of Callan–Symanzik-type for all fields,

$$\Delta S_k = \int_x \left[\frac{1}{2g^2} a_\mu^z k^2 a_z^\mu + \bar{c}_z k^2 c^z + c_\psi \bar{\psi} k \psi \right]. \quad (33)$$

The constant $c_\psi \in \mathbb{R}$ indicates the ratio of regularization scales between quarks and gluons or ghosts. We mostly set it to one in this work. This regulator piece acts as a mass term for all fields and has the following important properties:

1. It is local / momentum independent and invariant under Euclidean rotations.
2. It is invariant under background-field gauge transformations.
3. It is independent of the background field \bar{A} .

This leads to the w.r.t. the Renormalization Group (RG)-scale k dependent Schwinger functional W_k ,

$$\begin{aligned} W_k[\bar{\eta}, \eta, J, \bar{A}, \bar{\omega}, \omega] = & \ln \left[\int \mathcal{D}\bar{\psi} \mathcal{D}\psi \mathcal{D}a \mathcal{D}c \mathcal{D}\bar{c} \right. \\ & \exp \left(- (S + \Delta S_k)[\bar{\psi}, \psi, a, \bar{A}, \bar{c}, c] \right. \\ & \left. \left. + \int_x [\bar{\psi} \eta + \bar{\eta} \psi + J_z^\mu (\bar{A}_\mu^z + a_\mu^z) + \bar{c} \omega + \bar{\omega} c] \right) \right]. \end{aligned} \quad (34)$$

The so-called *effective average action* Γ_k is obtained by the Legendre transform of W_k and a subtraction of the regulator term, which is then given in terms of the field expectation values. After all calculations, we identify the background-field \bar{A} with the expectation value of the gauge field A as before,

$$\begin{aligned} \Gamma_k[\bar{\psi}, \psi, A, \bar{c}, c] & \quad (35) \\ = & \left[\sup_{\bar{\eta}, \eta, J, \omega, \bar{\omega}} \left(\int_x [\bar{\psi} \eta + \bar{\eta} \psi + J_z^\mu (\bar{A}_\mu^z + a_\mu^z) + \bar{c} \omega + \bar{\omega} c] \right. \right. \\ & \left. \left. - W_k[\bar{\eta}, \eta, J, \bar{A}, \bar{\omega}, \omega] \right) - \Delta S_k[\bar{\psi}, \psi, a, \bar{A}, \bar{c}, c] \right]_{\bar{A}=A, a=0}. \end{aligned}$$

This construction allows to study the theory at arbitrary mass scales k with the full quantum effective action Γ being recovered at $k = 0$. Crucially, the Osterwalder–Schrader axioms [62, 63] are satisfied by the regularized theory because of property 1. Hence, we can always perform a Wick rotation back to Minkowski spacetime and obtain a well-defined QFT at all scales k , where in particular Lorentz invariance, causality, and unitarity are fulfilled. Since the regulator piece has no momentum dependences, no additional poles are introduced in the propagators. They would complicate the analytic continuation

to Minkowski spacetime [64] which is connected to a possible breaking of Osterwalder–Schrader reflection positivity [65]. Besides, property 2 importantly ensures that the auxiliary symmetry under background-field gauge transformations remains intact for Γ_k . This leads to physical gauge invariance at $k = 0$ in the way described at the end of Section III B. However, one has to adapt how the regulator piece (33) affects the Ward identities introduced in the previous subsection III C. Recall that these are linked to fluctuation-field gauge-transformations.

It turns out that the Ward–Takahashi identity (28) remains valid at all scales for the mass-like regulator,

$$\mathcal{G}^z \Gamma_k = \langle \mathcal{G}^z (S_{\text{gf}} + S_{\text{gh}}) \rangle_J. \quad (36)$$

This remarkable result is derived in Appendix B. Even though a gluon mass term is not invariant under fluctuation-field gauge transformations, $\mathcal{G}^z \Delta S_k$ happens to be linear in the fluctuation fields only, and the symmetry is restored at all scales by removing the regulator term in Eq. (35). Equation (36) sets constraints on Γ_k , *e.g.* whether a gluon mass term may (not) appear. In general, the presence of a regulator modifies the identity, *c.f.* Eq. (B1).

The regulator piece breaks the BRST symmetry. Since this transformation is highly non-linear, the use of the local regulator (33) leads to a non-trivial modification of the Slavnov–Taylor identity (30). See Ref. [53, Eq. (78)] for a general expression of it, which is also called modified Quantum Master Equation.

Finally, property 3 guarantees that the Nielsen identity (32) holds for the effective average action, too. This statement,

$$\left. \frac{\delta \Gamma_k[a, \bar{A}]}{\delta \bar{A}} \right|_{a=a_{\text{eq}}} = 0, \quad (37)$$

again assumes an on-shell evaluation, *i.e.* a_{eq} is determined such that $(\delta \Gamma_k / \delta a)|_{a=a_{\text{eq}}} = 0$. At all scales k , Γ_k is on-shell independent of the choice for \bar{A} . Consequently, one may identify the background-field with the field expectation value not just at vanishing regulator with $k = 0$ but on-shell at arbitrary scales. Off-shell, there is a constraint on Γ_k , but it does not contain an explicit scale-dependence via the regulator, *c.f.* Eq. (C9). The r.h.s. of Eq. (37) is non-zero for arbitrary regulators, *c.f.* Eq. (C6).¹

To summarize, the local regulator piece (33) regularizes the IR-divergencies of the theory and keeps its analytic structure without violating gauge-invariance and background-field independence in the sense of Eqs. (36) and (37). These are very special properties of the regulator. Identities related to the latter two would drastically

simplify without the need of the gauge-fixing and ghost terms at all in the action.

IV. THE METHOD: THE FRG

We need a nonperturbative approach to investigate the infrared properties of the model and in particular its low-energy degrees of freedom. We use the exact, nonperturbative FRG flow equation [66–68], which is also denoted as Wetterich equation or Exact Renormalization Group (ERG) equation,

$$k \partial_k \Gamma_k[\Phi] = \frac{1}{2} \text{STr} \left((k \partial_k R_k) (\Gamma_k^{(2)} + R_k)^{-1}[\Phi] \right). \quad (38)$$

It contains a super-trace over all fields of the theory, being collected in an abstract field vector Φ and taken to be fixed bare fields, and also accounts for the Grassmann property for fermions. We refer again to Ref. [30, App. F] for our conventions, see also Refs. [69–71]. For details on the FRG, we refer to Refs. [53, 59, 72, 73].

From now on, we emphasize that the regulator function R_k is supposed to satisfy the usual regulator properties [59, Eqs. (13)–(15)] which is the case for the momentum independent regulator (33). For a detailed discussion on choices of regulators, we refer to Refs. [64, 70, 74–83].

The main advantages of Callan–Symanzik-type regulators for our study are given by the properties 1 to 3. Problems with UV divergencies might only occur in case of an ansatz for the effective average action Γ_k by means of a truncation that introduces local, dimensionless couplings. We discuss partial bosonization as a solution to this problem with local, four-fermion interaction vertices in the discussion and outlook.

The price to be paid with the choice of the fermion regulator is that it obviously breaks chiral symmetry in the limit where quarks are massless. It implies that the limit of zero quark mass must be taken very carefully in all expressions. One should also not forget that physical interpretations are, strictly speaking, only possible at $k = 0$ where all symmetries are restored. It is the truncation that we need to apply to the effective action that possibly leads to regulator dependent results.

V. QUANTUM EFFECTIVE ACTION: MINIMAL ANSATZ

We must make an ansatz for the effective action for explicit calculations with the Wetterich equation. In this section, we stay close to the perturbative setup and solely introduce a scale-dependent gauge coupling, fermion mass, and wave-function renormalization that evolve during the RG flow starting off from the classical action. Later on, we will significantly extend this truncation. We start our discussion with the derivation of the corresponding flow equations. Afterwards we discuss their solution and interesting limits.

¹ Note that there seems to be sign mistake in Ref. [53, Eq. (79)], which is why we re-derive the expression in Appendix C. There, we also explain the on-shell evaluation of the resulting expression.

A. A minimal truncation

There are various approximation schemes used in the literature such as expanding the effective action in terms of vertices or field derivatives as well as combinations thereof [53, 59, 70, 72, 73]. The ansatz should always be compatible with the microscopic action such that one can formulate the initial conditions for its scale-dependent quantities. In this section, we opt for a truncation to lowest order in fields and derivatives,

$$\begin{aligned} & \Gamma_k[a, A = \bar{A} + a, \bar{\psi}, \psi, \bar{c}, c] \\ &= \int_x \left(\bar{\psi} (\gamma^\mu D_\mu[A] + m) \psi + \frac{1}{4g^2} F_{\mu\nu}^z F_z^{\mu\nu} \right. \\ & \quad \left. - \frac{1}{2\xi} a_\mu^\mu D_\mu^z[\bar{A}] D_{\nu\nu}^w[\bar{A}] a^{\nu\nu} - \bar{c}_z D_\mu^z[\bar{A}] D^{\mu w}_v[A] c^v \right). \end{aligned} \quad (39)$$

It essentially mimics the microscopic gauge-fixed action, but the gauge coupling g and the fermion mass m are scale-dependent and take their bare values in the UV. Furthermore, we work with renormalized fields that implicitly contain a scale dependence via a wave-function renormalization factor Z that is initialized at one in the UV and absorbed into the fields,

$$\Phi \equiv (A, \sqrt{Z_\psi} \psi, \sqrt{Z_\psi} \bar{\psi}, c, \bar{c}). \quad (40)$$

As we will see, it is an approximation to not take a ghost wave-function renormalization into account, while it stays an exact statement for the gluon field with a running coupling in our convention as long as gauge invariance holds, see Appendix D. Functional derivatives are always taken w.r.t. renormalized fields. The Wetterich equation consequently receives a modification when the renormalized fields are held fixed while taking the scale-derivative,

$$k \partial_k \Gamma_k - \frac{1}{2} \eta_{\mathbf{a}} \Phi_{\mathbf{a}} \frac{\delta \Gamma_k}{\delta \Phi_{\mathbf{a}}} = \frac{1}{2} \text{STr} \left(\frac{k \partial_k R_k - \eta R_k}{\Gamma_k^{(2)} + R_k} \right). \quad (41)$$

Here, we introduced the anomalous dimension

$$\eta_\psi \equiv -k \partial_k \ln Z_\psi, \quad (42)$$

implicitly sum over the field-space vector index \mathbf{a} and assume that the regulator piece $\Delta S_k[\Phi]$ is given in terms of renormalized fields. It is oftentimes useful to again rewrite Eq. (41) into the form

$$k \partial_k \Gamma_k - \frac{1}{2} \eta_{\mathbf{a}} \Phi_{\mathbf{a}} \frac{\delta \Gamma_k}{\delta \Phi_{\mathbf{a}}} = \frac{1}{2} \text{STr} \left(k \tilde{\partial}_k (\ln \mathcal{P}_k) \right) \quad (43)$$

by introducing the derivative $\tilde{\partial}_k$, which is supposed to exclusively act on the regulator insertion, as well as the full two-point function

$$\mathcal{P}_k[\Phi] = (\Gamma_k^{(2)} + R_k)[\Phi]. \quad (44)$$

This also allows direct comparison with the perturbative one-loop correction to the effective action and reduces computational complexity in the nonperturbative setup.

Finally, we also introduce the RG-time t as

$$\partial_t = -k \partial_k, \quad t = -\ln(k/\Lambda) \in [0, \infty), \quad (45)$$

which is chosen to be positive for the RG flow from the UV reference scale Λ to the IR.

The third term in the ansatz (39) stems from the gauge fixing and we work in Feynman-'t Hooft gauge $\xi = 1$ within the present work. We plan to investigate the gauge-dependence in future studies. After all calculations, one has to evaluate the action at its field expectation values to obtain the effective action.

The strategy to derive flow equations for the scale-dependent parameters is as follows: By taking functional derivatives of the Wetterich equation one obtains an expression for the RG-time-derivative of an n -point vertex function which can be computed via the r.h.s. in terms of a loop expression. Then one extracts the flow of each scale-dependent parameter via specific projections. In practice, it is useful to do all computations in momentum space. Corresponding conventions for Fourier transformations can be found in Ref. [30, App. C]. There, we also list all momentum-space expressions for the n -point vertex functions and full propagators that are used during these calculations and that are computed from the ansatz (39).

B. Running quark mass and wave function

First, we derive equations for m and η_ψ by taking two functional derivatives of the Wetterich equation (41) w.r.t. the fermionic fields. The resulting expression for the fermion two-point vertex function can be depicted in terms of Feynman diagrams as

$$\partial_t \longrightarrow \text{---} \circ \text{---} \quad (46)$$

$$= \text{---} \circ \text{---} + \text{---} \circ \text{---},$$

where the external lines are drawn for visualization purposes only and the regulator insertion is indicated by a crossed circle. Gluon propagators are depicted as curly lines and fermion propagators as solid lines with arrows. One has to project both sides of Eq. (46) on the mass and kinetic term in order to extract flow equations for m and η_ψ , respectively. A detailed derivation is given in Ref. [30, App. G].

It turns out that the anomalous dimension vanishes for our choice of gauge fixing and we arrive at

$$\eta_\psi = 0. \quad (47)$$

Besides, it is convenient to introduce dimensionless quantities

$$\tilde{g} = \frac{g}{k}, \quad \tilde{m} = \frac{m}{k}. \quad (48)$$

For the sake of better readability, we also provide the following relations,

$$\partial_t \tilde{m} = -\partial_k m + \frac{m}{k}, \quad \partial_t \tilde{g} = -\partial_k g + \frac{g}{k}, \quad (49)$$

$$k \partial_k \left(\frac{k^2}{g^2} \right) = 2 \frac{k^2}{g^2} \left(1 - \frac{k}{g} \partial_k g \right) = 2 \frac{k^2}{g^2} \left(\partial_t \ln \tilde{g} \right). \quad (50)$$

Using this notation we obtain the final result for the flow of the fermion mass for $c_\psi = 1$,

$$\begin{aligned} & \partial_t \tilde{m} - \tilde{m} + \eta_\psi \tilde{m} \\ &= \frac{(N_c^2 - 1) \tilde{g}^2}{2 \pi N_c \tilde{m}^2 (2 + \tilde{m})^2} \left(-\tilde{m} (2 + \tilde{m}) [1 - \eta_\psi \right. \\ & \quad \left. - (1 + \tilde{m}) (\partial_t \ln \tilde{g})] + [-2 (\partial_t \ln \tilde{g}) (1 + \tilde{m}) \right. \\ & \quad \left. - (2 + \tilde{m} (2 + \tilde{m})) (-1 + \eta_\psi)] \ln(1 + \tilde{m}) \right). \end{aligned} \quad (51)$$

Note that the t -derivatives of the gauge coupling on the r.h.s. stem from the dependence of our regulator insertion on the gauge coupling, see Eqs. (33) and (50). The prefactor $(N_c^2 - 1)/N_c$ is expected because the $N_c^2 - 1$ gluons that contribute to the r.h.s. of Eq. (46) must be distributed over the N_c color charges carried by the fermions.

C. Running gauge coupling

We use Eq. (43) to compute the flow of the gauge coupling. This is similar to the perturbative approach, see, *e.g.*, Ref. [52, Sec. 16.6], and we basically follow these steps applied to the FRG formalism. The logarithm generates terms of all orders in the background gauge field that are allowed by symmetries. The part that is relevant to us is the lowest order background gauge-invariant contribution $\text{tr}(\bar{F}_{\mu\nu} \bar{F}^{\mu\nu})$ which is part of our ansatz. We choose to project onto the part that is quadratic in the background-field \bar{A} . Both sides of the flow equation can then again be represented by Feynman diagrams as

$$\begin{aligned} & \partial_t \text{ooooo} = \\ &= \text{ooooo} \text{ooooo} - \frac{1}{2} \text{ooooo} \text{ooooo} + \\ & \quad - 2 \text{ooooo} \text{ooooo} + \text{ooooo} \text{ooooo} \end{aligned} \quad (52)$$

$$- N_f \text{ooooo} \text{ooooo} + \frac{N_f}{2} \text{ooooo} \text{ooooo}.$$

Strictly speaking, the quark field has no fundamental vertex that would allow for a ‘‘tadpole’’-type diagram. It arises from rewriting

$$\begin{aligned} & \text{Tr} \left(\ln [\gamma^\mu D_\mu + m + k] \right) \\ &= \frac{1}{2} \ln \left(\text{Det} [-D^2 + (m + k)^2 + i [D_\mu, D_\nu] \frac{i}{4} [\gamma^\alpha, \gamma^\beta]] \right), \end{aligned} \quad (53)$$

where the covariant derivative is w.r.t. the background field. For details of this procedure we refer to Ref. [30, App. G], where furthermore the computation without this rewriting is presented. The advantage is, however, that using Feynman–t Hooft gauge, $\xi = 1$, we can treat all three contributions in the same way in terms of a generalized d’Alembert operator,

$$\mathcal{P}_{(s)}^{(r)} = -\mathbb{1}_{(s)} D^{(r)} [\bar{A}]^2 + \bar{F}_{\alpha\beta}^{(r)} J_{(s)}^{\alpha\beta}. \quad (54)$$

These simplifications are the main advantages of this gauge. The index (s) indicates the spin of the field in the field space vector and $J_{(s)}$ its generator of Lorentz transformations,

$$(J_{(1)}^{\alpha\beta})^{\mu\nu} = i (\delta^{\alpha\mu} \delta^{\beta\nu} - \delta^{\alpha\nu} \delta^{\beta\mu}), \quad (55)$$

$$(J_{(\frac{1}{2})}^{\alpha\beta})^a_b = \frac{i}{4} [\gamma^\alpha, \gamma^\beta]^a_b. \quad (56)$$

The gauge-group representation of the background-field \bar{A} is denoted by (r) , but we can already identify \bar{A} with the full field A . The last term in Eq. (54) describes the magnetic-moment interaction with the gauge field. It is the only term from the purely gauge-field ‘‘dynamics’’ that contributes to the flow of the gauge coupling in 1 + 1 dimensions. Its overall contribution from the minimal coupling, which is given by the square of the covariant derivative, vanishes. This is because the ghost contribution exactly cancels the gluon contribution, as it should be for the unphysical longitudinal gluon modes and there are no transversal modes in 1 + 1 dimensions. The explicit calculation is provided in Ref. [30, App. G]. We want to highlight that the gauge invariant tensor structure of the form $(p^2 \delta^{\mu\nu} - p^\mu p^\nu)$ is indeed preserved on both sides of the flow Eq. (52). While the ‘‘tadpole’’-type diagram does not contribute to the flow of the gauge coupling it is needed to preserve this gauge invariant tensor structure.

In the end, after adding up all contributions we find

$$\partial_k g = -\partial_t \tilde{g} + \tilde{g} = -\tilde{g}^3 \frac{\frac{N_c}{\pi} - \frac{N_f}{12\pi} \frac{(1-\eta_\psi)}{(1+\tilde{m})^3}}{1 - \frac{11}{12} \frac{N_c}{\pi} \tilde{g}^2} \quad (57)$$

for the flow equation of the gauge coupling. Here, we already used $c_\psi = 1$ and switched to dimensionless quantities Eqs. (48) to (50). For general c_ψ , we refer to Ref. [30, Eq. (G.37)].

Before we study solutions of the flow equation a few remarks are in order: we recover the perturbative one-loop result for the flow of the gauge coupling which is the term at leading order in \tilde{g} . The negative sign tells that the gauge coupling increases towards lower scales as expected. Besides, we obtain some parts of the higher-loop contributions by expanding the denominator. But of course, there are more terms in the effective action that also contribute at higher order. Examples are terms of higher order in the field-strength tensor or a ghost wave-function renormalization. The pole in the denominator already signals a breakdown of our truncation.

D. Consistency check: the quark-gluon vertex

Gauge invariance sets a constraint on the flow of the quark-gluon-vertex. Here, we show that it is indeed satisfied and even in a very convenient way for the particular gauge $\xi = 1$. The constraint can be checked by taking functional derivatives of the Wetterich equation w.r.t. the gluon field and the fermion fields, which diagrammatically reads

$$\partial_t \text{ (vertex) } = \text{ (triangle loop diagrams) } + \dots, \quad (58)$$

where the dots indicate the other possible regulator insertions. The projection of the left hand side (l.h.s.) of Eq. (58) onto the quark-gluon-vertex must be proportional to the anomalous dimension of the fermions by construction of the covariant derivative in Eq. (3), see also Appendix D. Since it is zero for the gauge $\xi = 1$, the r.h.s. must vanish as well which is indeed the case. Hence, the constraint is automatically satisfied.

E. Limiting cases

In this section, we study the flow equations for the mass and gauge coupling in interesting limits. In agreement with the ansatz we only consider contributions up to order \tilde{g}^2 . All higher orders are a consequence of the regulator choice for the fluctuating gluon field, see Eqs. (33) and (50). Hence, we take the denominator to

be one in Eq. (57) and simplify by setting $(\partial_t \ln \tilde{g}) \rightarrow 1$ in Eq. (51).² Furthermore, the anomalous dimension for the fermions η_ψ vanishes, Eq. (47), hence the wave-function renormalization factor is equal to one at all scales, and we work with

$$\partial_t \tilde{g} - \tilde{g} = -\partial_k g \quad (59)$$

$$= \tilde{g}^3 \left(\frac{N_c}{\pi} - \frac{N_f}{12\pi} \frac{1}{(1 + \tilde{m})^3} \right),$$

$$\partial_t \tilde{m} - \tilde{m} = -\partial_k m \quad (60)$$

$$= \frac{(N_c^2 - 1) \tilde{g}^2}{2\pi N_c (2 + \tilde{m})^2} \frac{2c_\psi \ln c_\psi}{c_\psi^2 - 1} [2 + \tilde{m} + \ln(1 + \tilde{m})].$$

These equations are visualized as a flow-diagram in Fig. 2. Generally, such a representation is helpful to identify possible fixed points. We explain the two diagrams and their different regimes further in the subsequent sections.

1. Dynamics in the UV

Studying the model in the UV for large k is relevant because our truncation is expected to be valid in this regime, where the effective average action is supposed to be close to the microscopic action. Here, we can analyze how the parameters start to flow due to the fluctuations on largest scales in momentum space. The limit is characterized by

$$\tilde{m}, \tilde{g} \ll 1. \quad (61)$$

It is practical to give the limit of Eqs. (59) and (60) in terms of the variables m , g and k ,

$$\partial_k g = -\frac{g^3}{k^3} \bar{n}, \quad (62)$$

$$\partial_k m = -\frac{2c_\psi \ln c_\psi}{c_\psi^2 - 1} \frac{(N_c^2 - 1)}{4\pi N_c} \frac{g^2}{k^2}. \quad (63)$$

Here, we (re)introduced the parameter c_ψ and defined

$$\bar{n} \equiv \frac{N_c}{\pi} - \frac{N_f}{12\pi c_\psi^2}, \quad (64)$$

in order to ease the notation. The flow of the gauge coupling is decoupled from the mass and its solution is

$$g = \frac{g_\Lambda}{\sqrt{1 - \bar{n} g_\Lambda^2 \left(\frac{1}{k^2} - \frac{1}{\Lambda^2} \right)}}. \quad (65)$$

² In fact, this simply corresponds to an expansion in g up to quadratic order.

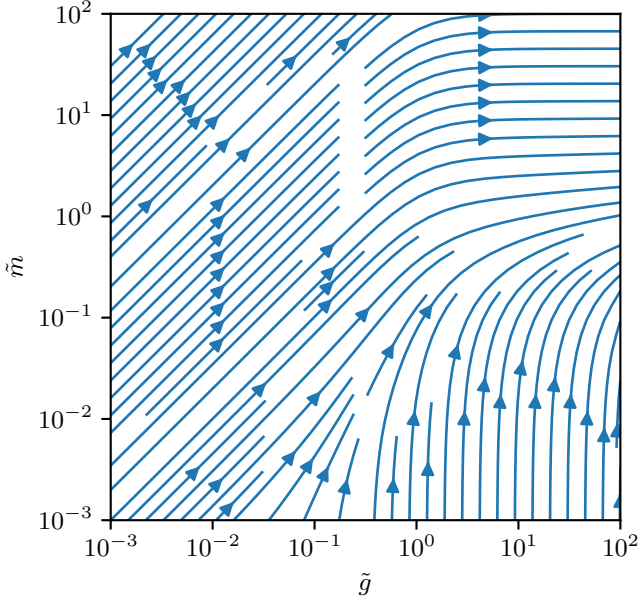
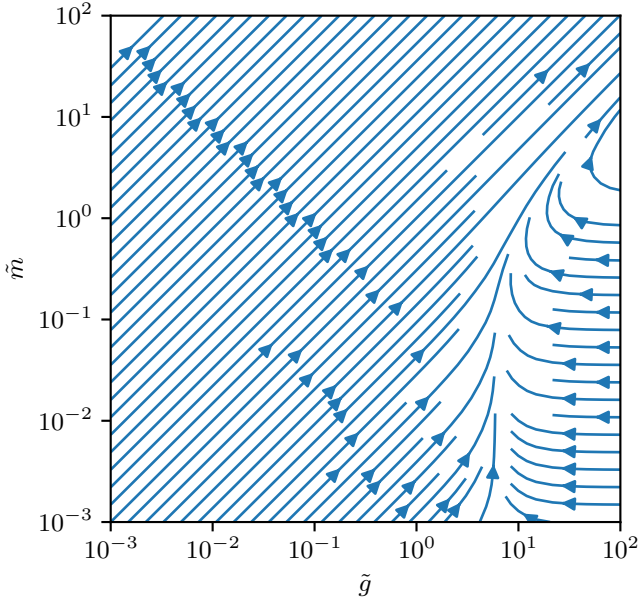
(a) Finite values $N_c = 3$, $N_f = 1$.(b) Infinite- N_f limit.

FIG. 2. Flow-diagram for the dimensionless gauge coupling \tilde{g} and fermion mass \tilde{m} in the \tilde{g} - \tilde{m} -plane. To take the infinite- N_f limit, we need to re-scale the quantities according to Eq. (83). For a given set of values, the arrows indicate the direction of their flow towards the IR.

Thereby, Λ is some UV scale and the limit $\Lambda \rightarrow \infty$ can be taken, the theory is super-renormalizable. The gauge coupling approaches a finite UV value. That the theory is not free in the UV is already clear from the linearly growing potential between quarks which is already present on the classical level as mentioned in Section II A. The flow equation for the fermion mass becomes soluble with the

result for the gauge coupling. We must distinguish according to the sign of \bar{n} :

1. For the gluon dominated case with $\bar{n} > 0$ we find

$$g = \frac{g_\infty}{\sqrt{1 - \bar{n} \frac{g_\infty^2}{k^2}}}, \quad (66)$$

$$m = m_\infty \quad (67)$$

$$+ \frac{N_c^2 - 1}{4\pi N_c} \frac{2c_\psi \ln c_\psi}{c_\psi^2 - 1} \frac{g_\infty}{\sqrt{\bar{n}}} \operatorname{arctanh}\left(\frac{\sqrt{\bar{n}} g_\infty}{k}\right),$$

where the UV scale is removed by $\Lambda \rightarrow \infty$, see Ref. [30, App. H] for an explicit derivation. The condition $\bar{n} > 0$ is certainly true for $N_c = 3$, $c_\psi \geq 1$ and $N_f \leq 6$ – values similar to QCD in four dimensions. It also means that the auxiliary parameter c_ψ may not take arbitrary values but gluonic and fermionic fluctuations should be introduced at roughly equal scales. As in four dimensions, the gauge coupling increases towards the IR and we observe that the gauge coupling develops a singularity, it becomes infinite, when the RG scale reaches the “model scale”,

$$k = \sqrt{\bar{n}} g_\infty. \quad (68)$$

The truncation breaks down at this scale at the latest and higher-order contributions in \tilde{g} become relevant. Taking all higher-order contributions of our simplistic result Eq. (57) into account we find that the gauge coupling increases even faster towards lower RG scales. It still develops a singularity with infinite derivative but g remains finite because the denominator in Eq. (57) approaches its root fast enough with growing \tilde{g} .

The mass also increases during the flow and develops a singularity at the same scale as the gauge coupling due to the direct dependence on the latter. This is independent from the initial value of the fermion mass. We emphasize that the growing mass in this limit is a feature of the quark regulator that acts as a mass and breaks chiral symmetry. Large values of k mean that fluctuating quarks are heavy and not that they have large momenta. A perturbative calculation with the diagrams shown in Eq. (46) using dimensional regularization does not give a growing mass starting with a massless theory because the projection on the Dirac unit matrix vanishes. Once $\tilde{m} \ll 1$ is violated we must use the full equation Eq. (51).

2. For the fermion dominated case with $\bar{n} < 0$ we still find

$$g = \frac{g_\infty}{\sqrt{1 - \bar{n} \frac{g_\infty^2}{k^2}}}, \quad (69)$$

while

$$m = m_\infty + \frac{N_c^2 - 1}{4\pi N_c} \frac{2 c_\psi \ln c_\psi}{c_\psi^2 - 1} \frac{g_\infty}{\sqrt{|\bar{n}|}} \times \left[\frac{\pi}{2} - \operatorname{arccot} \left(\frac{\sqrt{|\bar{n}|} g_\infty}{k} \right) \right], \quad (70)$$

where the UV scale was again removed $\Lambda \rightarrow \infty$. However, due to the sign-change of \bar{n} , instead of running into an IR divergence, the coupling decreases towards the IR and would be zero at $k = 0$, if the UV-limit was valid on all scales. Moreover, the fermion mass increases but approaches a finite IR value. In Section V E 3 we continue to discuss this case beyond the approximation of large k .

In any case, the UV-regime corresponds to the bottom left corners of the flow-diagrams in Fig. 2. The dimensionless quantities \tilde{g} and \tilde{m} are considered there and a 45° angle of the curves corresponds to the fact that the $1/k$ -dependence dominates their flow.

We finish the discussion by pointing out two more identities for later use that are valid at large RG scales in the UV

$$\eta_\psi \ll 1, \quad (71)$$

$$(\partial_t \ln \tilde{g}) = -\frac{1}{\tilde{g}} \partial_k \tilde{g} = 1 - \frac{k}{g} \partial_k g \stackrel{(59)}{\approx} 1. \quad (72)$$

The first equation is actually valid on all RG scales within our truncation. Moreover, it also holds for any truncation in the UV regime because it is at least of order \tilde{g}^2 and just gives a correction to $Z_\psi = 1$. Oftentimes, it is even a good approximation at smaller scales or in particular gauges [84–86]. The second identity reflects that the derivative of the fluctuating gluon regulator piece is mainly given by the derivative acting on the k^2 term and the factor $1/g^2$ just gives a correction, see also Eq. (50). We stress again that this approximation (72) is generally made to simplify the r.h.s. of the flow equations within the truncation in this work.

2. Large coupling and fermion mass

Let us return to the case $\bar{n} > 0$ and ask what actually happens to our full flow equations (59) and (60) when the gauge coupling and fermion mass both become large at some intermediate RG scale on their evolution to the IR. An increasing fermion mass in general implies a suppression of fermionic fluctuations which leads to a suppression of their contributions to the RG flow. In general, we find that the growth of g and m seem to be competing effects in Eq. (60).

Thus, assume we reached an regime, where $\tilde{g}, \tilde{m} \gg 1$ and $\eta_\psi \ll 1$ at some RG scale $k = \mu$. As a consequence,

the flow equations (59) and (60) can be approximated by

$$\partial_k g = -\tilde{g}^3 \frac{N_c}{\pi}, \quad (73)$$

$$\partial_k m = -\frac{N_c^2 - 1}{2\pi N_c} \frac{2 c_\psi \ln c_\psi}{c_\psi^2 - 1} \frac{\tilde{g}^2}{\tilde{m}}, \quad (74)$$

below this scale. Indeed, the fermionic contribution to the flow of the gauge coupling drops out and an analytic solution is available that again allows to solve the flow equation for the fermion mass. The solutions are

$$g^2 = \frac{g_\mu^2}{1 - c \left(\frac{\mu^2}{k^2} - 1 \right)}, \quad (75)$$

$$m^2 = m_\mu^2 - \frac{2 c_\psi \ln c_\psi}{c_\psi^2 - 1} \frac{N_c^2 - 1}{2\pi N_c (1 + c)} g_\mu^2 \times \ln \left(\frac{k^2}{\mu^2} \left[1 - c \left(\frac{\mu^2}{k^2} - 1 \right) \right] \right). \quad (76)$$

Here, we introduced

$$c \equiv \frac{N_c}{\pi} \frac{g_\mu^2}{\mu^2} \quad (77)$$

to ease the notation. Both quantities diverge in the limit $c \left(\frac{\mu^2}{k^2} - 1 \right) \rightarrow 1$, meaning that they diverge when k is lowered from μ to even smaller scales. In particular, we find

$$\lim_{c(\mu^2/k^2-1) \rightarrow 1} \frac{m^2}{\mu^2} = 0, \quad (78)$$

which means that the coupling grows faster than the fermion mass.

The discussion of this section corresponds to the top right corner of the flow-diagram in Fig. 2a. It appears as if \tilde{m} approaches a constant value while \tilde{g} increases, but this reflects that \tilde{g} increases much faster than \tilde{m} .

A plot of the numerical solution to the flow equations Eqs. (59) and (60) for the boson dominated case is given for the gauge coupling by the blue curve in Fig. 3.

3. Infinite- N_c limit

We emphasized already the importance of the sign of \bar{n} defined in Eq. (64) in the UV regime. Therefore, it is worthwhile to further discuss the model for a boson or fermion dominated theory. In this section, we study the former case. In particular the infinite- N_c limit, also known as the 't Hooft limit [7], is interesting. The implications for QCD are that only so-called “planar diagrams” contribute. More general, the limit establishes a connection to a mean-field theory where the fermions do not fluctuate. This statement must be understood in the following sense (quarks still carry a color index and their number grows with N_c): Not all diagrams with fermion

propagators drop out of the dynamics. Only those diagrams with a purely fermionic loop are suppressed. The limit is taken with $g^2 N_c$ held fixed and N_f kept finite. Formally, this can be achieved with a rescaling of the gauge coupling

$$g_{N_c} \equiv \sqrt{N_c} g \quad (79)$$

before taking the limit with g_{N_c} held fixed. From Eqs. (59) and (60) we obtain

$$\partial_k g_{N_c} = -\frac{1}{\pi} \tilde{g}_{N_c}^3, \quad (80)$$

for the RG flow of the gauge coupling and

$$\partial_t \tilde{m} - \tilde{m} = -\partial_k m \quad (81)$$

$$= \frac{2 c_\psi \ln c_\psi}{c_\psi^2 - 1} \frac{\tilde{g}_{N_c}^2}{2\pi} \frac{2 + \tilde{m} + \ln(1 + \tilde{m})}{(2 + \tilde{m})^2}$$

for the flow equation of the mass. The fermion contribution to the gauge coupling, that has a screening effect, drops out in this limit as expected because the diagrams in Eq. (52) with fermion loops are suppressed. This is similar to the scenario discussed previously, where fermion fluctuations were suppressed in the IR due to a rising fermion mass. The UV-solution Eq. (65) becomes exact with $\bar{n}_{N_c} = 1/\pi$

$$g_{N_c} = \frac{g_{N_c, \Lambda}}{\sqrt{1 - \bar{n}_{N_c} g_{N_c, \Lambda}^2 \left(\frac{1}{k^2} - \frac{1}{\Lambda^2}\right)}}. \quad (82)$$

The flow equation of the fermion mass does not change qualitatively. The diagrams survive in the limit even though there is a fermion propagator because the external legs are fermionic.

4. Large and infinite- N_f limit

Now, we turn to the fermion dominated case with $\bar{n} < 0$. Similarly, as discussed before, one can take the infinite- N_f limit by keeping $g^2 N_f$ fixed. Again the theory becomes a mean-field theory but this limit is stronger than the infinite- N_c limit because gluons do not carry a flavor index. Hence, all diagrams with an internal gluon propagator are suppressed. Formally, this limit is taken by rescaling the gauge coupling

$$g_{N_f} \equiv \sqrt{N_f} g \quad (83)$$

and after sending $N_f \rightarrow \infty$ with g_{N_f} held fixed we obtain for Eqs. (59) and (60)

$$\partial_k g_{N_f} = \tilde{g}_{N_f}^3 \frac{N_f}{12\pi} \frac{1}{(1 + \tilde{m})^3}, \quad (84)$$

$$\partial_k m = 0. \quad (85)$$

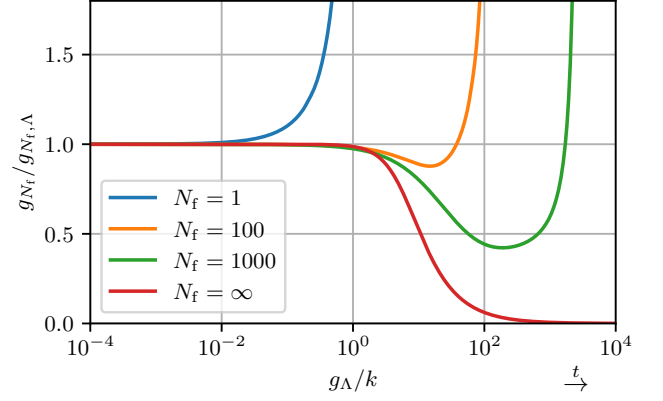


FIG. 3. Flow of the gauge coupling g_{N_f} for various flavors N_f . The UV values are $\Lambda/g_{N_f, \Lambda} = 10^5$ and $m_{\Lambda}/g_{N_f, \Lambda} = 10^{-3}$.

As expected, the only diagrammatic contribution that survives is the fermion loop contributing to the flow of the gauge coupling – here, the bosonic two-point function. The solutions to the infinite- N_f flow equations are

$$g_{N_f} = \frac{g_{N_f, \infty}}{\sqrt{1 + \frac{1}{12\pi} \frac{g_{N_f, \infty}^2}{m_{\infty}^2} \left(1 + \frac{k}{m_{\infty}}\right)^{-2}}}, \quad (86)$$

$$m = m_{\infty}. \quad (87)$$

Details on the derivation are given in Ref. [30, App. J]. The mass keeps its constant initial value because the gluon fluctuation in the fermion self energy is suppressed. The gauge coupling decreases and reaches a constant value

$$g_{N_f}(k=0) = \frac{g_{\infty}}{\sqrt{1 + \frac{1}{12\pi} \frac{g_{N_f, \infty}^2}{m_{\infty}^2}}}, \quad (88)$$

It approaches zero for $m_{\infty} \rightarrow 0$. A nonzero mass suppresses the IR fluctuations and the coupling remains finite. The solution of this limit is plotted in red in Fig. 3. It is remarkable that the coupling changes significantly over many orders of magnitude and one needs to resolve very low scales.

If N_f is large enough such that the gauge coupling decreases in the UV but N_f is taken to be finite there is a very different behavior, which is also shown in Fig. 3. The (generated) nonzero mass leads to a suppression of the fermion contribution to the gauge coupling towards the IR and the derivative of the coupling changes its sign, see Eq. (60) for $\tilde{m} \rightarrow \infty$. Therefore, the gauge coupling increases and eventually diverges as discussed in Section V E 2. The solution given in Eqs. (85) and (88) acts as a partial fixed point such that the divergence is shifted to lower scales.

The large- N_f limit is depicted in Fig. 2b. That the arrows take a 45° angle for large values can be explained as follows: even though the dimensionful quantities remain finite, the dimensionless quantities grow as $k \rightarrow 0$ and it is again the $1/k$ -dependence that dominates as in the UV-regime.

F. Summary of the chapter

To summarize, starting from the finite values of a super-renormalizable theory in the UV, the gauge coupling increases due to gluon fluctuations and decreases due to fermionic contributions towards the IR while the fermion mass never decreases during the flow. However, coupling and fermion mass always become infinite at a scale $k \simeq g_\Lambda$ at finite N_f where the coupling grows much faster than the mass. In the infinite- N_f limit, the gauge coupling decreases, the limit $k \rightarrow 0$ formally can be taken and approaches zero for decreasing initial mass.

The results of this section, in particular the increasing gauge coupling in the IR, suggest to continue the work in two directions. One step is to improve the truncation in the gauge sector of the effective action to reliably access the regime $k \simeq g_\Lambda$. We need to understand better how what is known about two-dimensional Yang–Mills theory, see Section IA, translates into the formulation we use here. Another possibility is to take higher orders in the fermionic field into account which are driven by the gauge coupling and therefore become very relevant on scales $k \simeq g_\Lambda$. As a first step, we continue with the latter investigation in the next section, which also constitutes a first step in the direction of our overall goal – obtaining a deeper understanding of dynamical hadronization.

VI. (LOCAL) FOUR-FERMION INTERACTIONS

Quantum fluctuations can dynamically generate effective couplings of all types, as long as these are compatible with the symmetries of the model. This comprises also those vertices that are not present in the microscopic action. Here, we investigate four-fermion interactions that are directly generated from the fermion-gluon interaction, see Fig. 4. From a perturbative point of view, they are the first new interactions that are generated in an expansion in the gauge coupling. Based on the previous discussion, they are expected to become relevant at scales $k \simeq g_\Lambda$ in $1 + 1$ spacetime dimensions.³ They are also important to find the emergent IR degrees of freedom, because resonant four-fermion channels are associated with the formation of mesonic bound states. In this

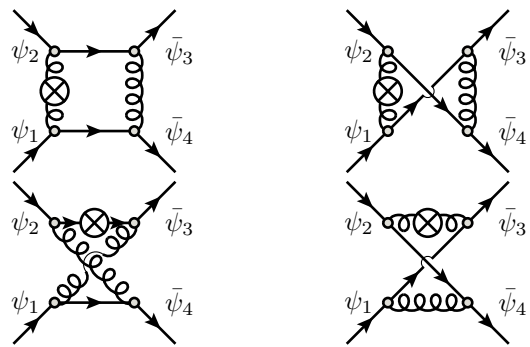


FIG. 4. Box-diagrams contributing to the flow of the four-fermion couplings. One representative regulator insertion is exemplarily drawn for each diagram.

section, we add them to the ansatz of the quantum effective action (39), derive and solve flow equations for the corresponding couplings. This is the first step to be made to discuss confinement and mesonic bound states. We remark that the Schwinger model usually is taken to be the prototype model for two-dimensional gauge theories with the property of a linearly rising Coulomb potential [3]. However, the mesonic bound state structure is much richer in QCD_2 – at least for $N_c \rightarrow \infty$, which makes this model extremely interesting.

At this point we again emphasize that we are of course not the first to study four-fermion interactions in the context of (models for) QCD. There are many works on four-fermion theories (in infinite- N limits) in $(1 + 1)$ -dimensions, which mostly emerged from original works by W. E. Thirring [87], D. J. Gross and A. Neveu [88] et al. and resulted in a variety of works on bound states, e.g. Refs. [89, 90], or the phase structure of these models at nonzero temperature and densities, e.g. Refs. [89, 91–93]. Also in $3 + 1$ dimensions four-fermion models have been studied extensively to model the strong interaction at low energies. Initially, concepts from solid state theory were transferred to particle physics by Y. Nambu and G. Jona-Lasinio [94, 95] to study chiral symmetry breaking. J. Braun et al. [96–98] studied four-fermion interactions in the context of QCD in $3 + 1$ dimensions in a Fierz-complete basis. Other related works in the FRG framework are Refs. [99–104]. However, we are not aware of a study similar to ours, where the emergence of four-fermion interactions is studied in a gauge theory in $1 + 1$ dimensions.

A. Extended truncation

We improve the minimal ansatz for the quantum effective action (39) from the previous section by including local, momentum-independent fermion interaction terms. We restrict ourselves to one flavor, $N_f = 1$. The restriction to pointlike interactions without momentum dependence is a severe approximation to describe the

³ This is different to $3 + 1$ dimensional QCD, because there the gauge coupling is dimensionless while the four-fermion couplings have nontrivial energy dimension.

IR physics as we will discuss later. However, to make progress and in a first step, we add the terms

$$\begin{aligned}
& -\frac{1}{N_c} \int_x \left[\frac{1}{2} \left(\lambda_1 (\bar{\psi} \psi)^2 + \lambda_2 (\bar{\psi} \gamma^{\text{ch}} \psi)^2 + \lambda_3 (\bar{\psi} \gamma^\mu \psi)^2 \right) \right. \\
& + \lambda_4 (\bar{\psi} T_z \psi)^2 + \lambda_5 (\bar{\psi} \gamma^{\text{ch}} T_z \psi)^2 + \lambda_6 (\bar{\psi} \gamma^\mu T_z \psi)^2 \\
& + \frac{1}{2} \left(\lambda_7 (\psi^{\text{T}} \mathcal{C} \psi)^{(cd)} (\bar{\psi} \mathcal{C} \bar{\psi}^{\text{T}})_{(dc)} \right. \\
& + \lambda_8 (\psi^{\text{T}} \mathcal{C} \gamma^{\text{ch}} \psi)^{[cd]} (\bar{\psi} \gamma^{\text{ch}} \mathcal{C} \bar{\psi}^{\text{T}})_{[dc]} \\
& \left. \left. + \lambda_9 (\psi^{\text{T}} \mathcal{C} \gamma^\mu \psi)^{[cd]} (\bar{\psi} \gamma^\mu \mathcal{C} \bar{\psi}^{\text{T}})_{[dc]} \right] \right] \quad (89)
\end{aligned}$$

to the ansatz for the effective action in Eq. (39). The matrix γ^{ch} is the two-dimensional analogue to the (3+1)-dimensional γ^5 and defined in terms of the Euclidean gamma-matrices as

$$\gamma^{\text{ch}} \equiv -\frac{i}{2} \epsilon_{\mu\nu} \gamma^\mu \gamma^\nu \equiv -i \gamma^0 \gamma^1, \quad (90)$$

where $\epsilon_{\mu\nu}$ is anti-symmetric with $\epsilon^{01} = \epsilon_{01} = 1$. We note the following special relation in two dimensions

$$\bar{\psi} \gamma^{\text{ch}} \gamma^\mu \psi = i \epsilon^{\mu\nu} \bar{\psi} \gamma_\nu \psi. \quad (91)$$

Besides, \mathcal{C} is the charge conjugation operator, see Ref. [30, App. A] for an explicit representation. The (anti-)symmetrization of the color indices is denoted by (square) round brackets, *e.g.*

$$(\psi^{\text{T}} \mathcal{C} \psi)^{(cd)} \equiv \frac{1}{2} \left[(\psi^c)^{\text{T}} \mathcal{C} \psi^d + (\psi^d)^{\text{T}} \mathcal{C} \psi^c \right]. \quad (92)$$

These bilinear combinations span all four-fermion interaction channels that are compatible with the symmetries and we introduced coupling constants $\{\lambda_i\}$ that are dimensionless,

$$[\lambda_i] = E^{2-d} \stackrel{d=2}{=} E^0. \quad (93)$$

The bilinears in the first three terms with λ_1 , λ_2 and λ_3 are in the color singlet representation of the gauge group, those with λ_4 , λ_5 and λ_6 transform in the adjoint representation and the last three terms with λ_7 , λ_8 and λ_9 correspond to diquark interactions. The diquarks transform in the symmetric or anti-symmetric tensor representation of $SU(N_c)$. See Table I for an overview of further bilinear symmetry properties and Ref. [30, App. B] for a detailed discussion.

The nine interaction channels, which one naively writes down to cover all possible four-fermion interactions, form an ‘‘overcomplete basis’’ (in the pointlike limit) and the single terms are actually related by Fierz transformations, see Ref. [30, App. B] for details. The minimal set

TABLE I. Transformation behavior of quark bilinears of mass dimensions ($[\text{dim}]$) E^2 and E^1 under Lorentz transformations (L), charge conjugation (\mathcal{C}), parity (\mathcal{P}), time reversal (\mathcal{T}) and $U(1)_{\text{V/A}}$ phase transformations. $(-)\text{0}$ is a (pseudo)-scalar, $(-)\text{1}$ is a (pseudo)-Lorentz vector, $-/+$ means transformation into itself with negative/positive sign, \leftrightarrow is a mapping into partner diquark-bilinear, $\checkmark(\boldsymbol{\times})$ means that it is (not) invariant.

bilinear	[dim]	L	\mathcal{C}	\mathcal{P}	\mathcal{T}	\mathcal{CPT}	$U(1)_{\text{V}}$	$U(1)_{\text{A}}$
$\bar{\psi} \gamma^\mu \partial_\mu \psi$	E^2	0	+	0	0	+	\checkmark	\checkmark
$\bar{\psi} \partial_\mu \psi$	E^2	1	-	1	1	-	\checkmark	$\boldsymbol{\times}$
$\bar{\psi} \gamma^{\text{ch}} \partial_\mu \psi$	E^2	1	+	-1	-1	-	\checkmark	$\boldsymbol{\times}$
$\bar{\psi} \gamma^{\text{ch}} \gamma^\mu \partial_\mu \psi$	E^2	1	+	-0	-0	+	\checkmark	\checkmark
$\bar{\psi} \gamma^\mu \psi$	E^1	1	-	1	1	+	\checkmark	\checkmark
$\bar{\psi} \psi$	E^1	0	+	0	0	+	\checkmark	$\boldsymbol{\times}$
$\bar{\psi} \gamma^{\text{ch}} \psi$	E^1	0	-	-0	-0	-	\checkmark	$\boldsymbol{\times}$
$\bar{\psi} \gamma^{\text{ch}} \gamma^\mu \psi$	E^1	0	-	-1	-1	+	\checkmark	\checkmark
$\bar{\psi} \gamma^\mu \mathcal{C} \bar{\psi}^{\text{T}},$ $\psi^{\text{T}} \mathcal{C} \gamma^\mu \psi$	E^1	1	$-\leftrightarrow$	-1	-1	\leftrightarrow	$\boldsymbol{\times}$	$\boldsymbol{\times}$
$\bar{\psi} \mathcal{C} \bar{\psi}^{\text{T}},$ $\psi^{\text{T}} \mathcal{C} \psi$	E^1	0	$-\leftrightarrow$	-0	-0	$-\leftrightarrow$	$\boldsymbol{\times}$	\checkmark
$\bar{\psi} \gamma^{\text{ch}} \mathcal{C} \bar{\psi}^{\text{T}},$ $\psi^{\text{T}} \mathcal{C} \gamma^{\text{ch}} \psi$	E^1	0	$-\leftrightarrow$	0	0	$-\leftrightarrow$	$\boldsymbol{\times}$	\checkmark
$\bar{\psi} \gamma^{\text{ch}} \gamma^\mu \mathcal{C} \bar{\psi}^{\text{T}},$ $\psi^{\text{T}} \mathcal{C} \gamma^\mu \gamma^{\text{ch}} \psi$	E^1	1	$-\leftrightarrow$	1	1	\leftrightarrow	$\boldsymbol{\times}$	$\boldsymbol{\times}$

that forms a Fierz-complete basis is given by three channels, for instance those with the bilinears in the singlet or adjoint representation or the diquarks. We remark that if the four-fermion interactions are supposed to be invariant under chiral transformations, this sets additional constraints on the couplings. For instance, choosing the three bilinears in the singlet representation one requires $\lambda_1 = -\lambda_2$ to obtain the invariant subtraction

$$\frac{1}{2N_c} \left[(\bar{\psi} \psi)^2 - (\bar{\psi} \gamma^{\text{ch}} \psi)^2 \right]. \quad (94)$$

The vector channel λ_3 is invariant under chiral transformations on its own as can be seen by direct calculation or from the Fierz identities in Ref. [30, App. B].

B. Connection to other four-fermion models

The interaction term (94) characterizes what is in four dimensions nowadays called the Nambu–Jona–Lasinio (NJL) model [95]. It is a very popular model in the context of QCD for studying cold deconfined quark matter in an effective low-energy model. It can be generalized to N_f flavors with a continuous chiral symmetry [94], see also Refs. [100, 105–107]. The model is named NJL₂ [108] or chiral Gross–Neveu (GN) model in two dimensions. An

overview of different models is provided in Ref. [109]. D. J. Gross and A. Neveu proposed several models in two dimensions [88]. They also introduced the term with the coupling λ_1 , nowadays referred to as the interaction in the GN model in any number of dimensions. It has no mass term on the microscopic level as it is also the case for the NJL₂ model. In two dimensions, the GN model is interesting by itself because it shares some properties with (3 + 1)-dimensional QCD such as asymptotic freedom, dimensional transmutation and spontaneous (discrete) chiral symmetry breaking [110, Sec. I]. Lastly, the interaction term with λ_3 defines the Thirring model [87] originally studied for fermions only carrying Dirac indices where all three interaction terms are equivalent and

there is an analytical solution available. More remarks on purely fermionic theories are made in Section VID 3 in the limit of $g = 0$.

C. Deriving flow equations

Next, we study how these four-fermion interactions are dynamically generated by quantum fluctuations in the FRG formalism. To project onto these channels and to generate the corresponding flow equations, we first take functional derivatives of the Wetterich equation w.r.t. the fermion fields. The l.h.s. gives the flow of the full four-fermion vertex

$$\frac{(2\pi)^8 \delta^4(\partial_t \Gamma_k)}{\delta \bar{\psi}_{a_4 c_4 f_4}(-p_4) \delta \bar{\psi}_{a_3 c_3 f_3}(-p_3) \delta \psi^{a_2 c_2 f_2}(p_2) \delta \psi^{a_1 c_1 f_1}(p_1)} \Big|_{\bar{A}, a, \psi, \bar{\psi}, c, \bar{c} = 0} = \partial_t \begin{array}{c} \psi_2 \quad \bar{\psi}_3 \\ \psi_1 \quad \bar{\psi}_4 \end{array} \quad (95)$$

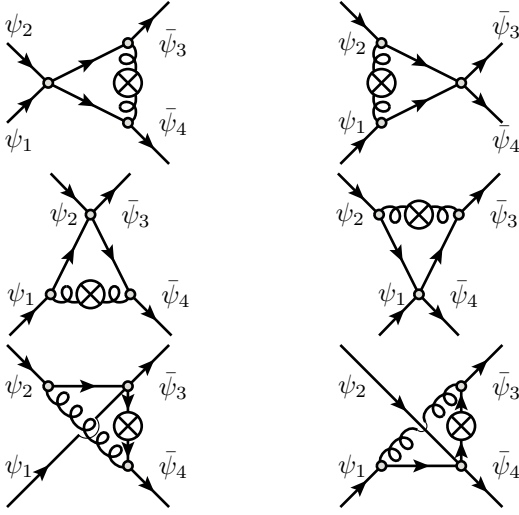


FIG. 5. Triangle-diagrams contributing to the flow of the four-fermion couplings. One representative regulator insertion is exemplary drawn for each diagram.

Its explicit form with its entire index structure is provided in Ref. [30, Eq. C.14]. The illustration of the r.h.s. in terms of Feynman diagrams is shown in Figs. 4 to 6. In general, we obtain 16 box-type diagrams, 18 triangular-type diagrams and 3 purely fermionic diagrams. The first ones are responsible for the initial generation of the effective couplings. The other diagrams become relevant once the four-fermion couplings are generated and then start feeding back into the flow.

There are two approaches to extract the flow equations

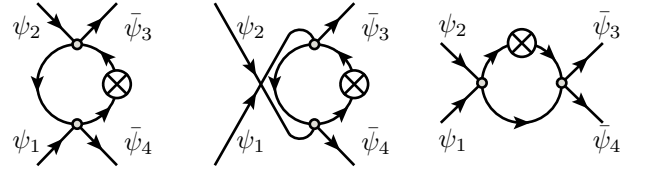


FIG. 6. Purely fermionic diagrams contributing to the flow of the four-fermion couplings. There are just three diagrams in total because regulator insertions in other internal lines lead to the same mathematical expression.

for the couplings from here.

a. Taking traces with subsequent matrix inversion
This approach makes use of computer program assistance. This is convenient since the number of diagrams is large and is even growing with every extension of the truncation. However, this approach allows to start with an overcomplete basis of interaction channels and to identify the Fierz-complete basis during the procedure. Hence, it does not require to work out the correct basis beforehand.

We proceed as follows. First, we make use of the DO-FUN [111] software package for MATHEMATICA [112] in order to take the functional derivatives of the flow equation. Then, we repeatedly contract the open indices with independent projectors using the FORMTRACER software [113]. One needs nine projectors starting off with the ansatz with nine couplings to end up with a system of nine equations that schematically looks like

$$M(\partial_t \lambda_1 + 2 \eta_\psi \lambda_1, \dots, \partial_t \lambda_9 + 2 \eta_\psi \lambda_9)^T = b. \quad (96)$$

Each row is the equation obtained from one projection, M encodes the pre-factors of the l.h.s. of the Wetterich equation and the vector b contains the projected loop expressions from the r.h.s. To disentangle the RG-time derivatives of the nine couplings $\partial_t \lambda_i$, $i \in \{1, \dots, 9\}$, on the l.h.s., one has to multiply the system of equations with the inverse of M . However, this is only possible if M is invertible which in turn is only possible if the interaction channels form a true basis. Hence, noninvertibility of M directly signals if channels in the ansatz are related by Fierz transformations. The rank of M determines the number of channels required for a Fierz-complete basis. We find that three are required for the symmetries of our model with $N_f = 1$, and we choose the channels with couplings λ_1 , λ_2 and λ_3 . The full flow equations are given in Ref. [30, App. I].

b. Expansion in tensor structure An alternative approach consists in expanding each loop expression in the tensor structure of the vertex which is only possible if one works with a Fierz-complete basis right from the start. In other words, every product of Dirac or color matrices must be expanded in its basis elements. In the end, one is able to compare both sides of the Wetterich equation and read off the flow equations for the couplings. This procedure is presented for the box-diagrams in Ref. [30, App. G] and was used as a crosscheck for the results obtained via the computer algebra tools. This method provides further understanding of the importance to make a Fierz complete ansatz.

We remark that some comparison of the projection and tensor basis approach was discussed and presented in talks already in the context of Refs. [96–98] but not reported on in detail. In general, we are not aware of a discussion of the reduction procedure of an “overcomplete basis” to a Fierz-complete basis in the context of the FRG via the Wetterich equation as it is used systematically in the present work.

D. Limiting cases

Similar to the previous section, we start our analysis of the RG flows with a discussion of particularly interesting limiting cases. First, we consider the UV limit, where the gauge coupling and fermion mass are assumed to be small compared to the RG scale. Afterwards, we discuss the full equations to then turn to the limit of vanishing gauge coupling as well as the infinite- N_c limit. The infinite- N_f limit cannot be discussed, because we already restricted ourselves to $N_f = 1$.

1. Dynamics in the UV

First of all, we investigate the UV regime as done for the minimal ansatz in Section VE 1. Here, we study how the four-fermion couplings are generated from the dynamics of the gauge sector. In particular, all contri-

butions from the triangle-diagrams and purely fermionic self interactions are irrelevant for the initial condition

$$\lim_{k \rightarrow \Lambda \rightarrow \infty} \lambda_i(k) = 0, \quad i = 1, 2, 3. \quad (97)$$

The contributions from the box-diagrams simplify significantly in the UV-limit. For details on the calculations we again refer to Ref. [30, App. I]. Remember that the latter limit is formally given by Eqs. (61), (71) and (72). Ultimately, we find

$$\partial_t \lambda_1 = \frac{\tilde{g}^4 (N_c [4 - (N_c - 2) N_c] + 4)}{12 \pi N_c}, \quad (98)$$

$$\partial_t \lambda_2 = \frac{\tilde{g}^4 [4 - N_c (3 N_c + 2)]}{12 \pi}, \quad (99)$$

$$\partial_t \lambda_3 = \frac{\tilde{g}^4 (N_c + 4)}{12 \pi}. \quad (100)$$

All three four-fermion couplings are generated from the gluon-exchange diagrams but have different flow equations. Still, the only differences are the prefactors a_i and the general form of the flow equations is

$$\partial_t \lambda_i = a_i \tilde{g}^4, \quad (101)$$

which is expected. Axial symmetry of our theory on all scales would require $a_1 = -a_2$ to ensure that only the symmetry preserving interaction, see Eq. (94), is generated in addition to the coupling λ_3 . As can be seen from the prefactors, this is not the case already in the UV, which implies that chiral symmetry – despite being a symmetry of the path integral – seems to be broken by the RG flow equations. In fact, we trace this symmetry breaking back to the choice of the fermion regulator in Eq. (33), which breaks chiral symmetry explicitly. We come back to this regulator feature below.

However, using the UV-solution to the gauge coupling, Eq. (65), we can analytically integrate Eq. (101) and find

$$\begin{aligned} \lambda_i &= -\frac{a_i}{2 \bar{n}^2} \left[\left(1 - \frac{k^2}{\bar{n} g_\infty^2} \right)^{-1} - \ln \left(1 - \frac{\bar{n} g_\infty^2}{k^2} \right) \right] \\ &= \frac{a_i}{4} \frac{g_\infty^4}{k^4} + \mathcal{O} \left(\frac{g_\infty^6}{k^6} \right), \end{aligned} \quad (102)$$

where the limit $\Lambda \rightarrow \infty$ is implied. The couplings are driven by the gauge coupling and start to grow significantly once the scale k reaches the scale of the gauge coupling in the UV, g_∞ . If this solution was valid on all scales, the couplings would become infinite in the limit $k^2 / (\bar{n} g_\infty^2) \rightarrow 1$ where the gauge coupling diverges. However, the equations are of course no longer valid in this regime.

2. Full equations

To obtain the full solution to our system of flow equations, see again Ref. [30, App. I], including the flow equa-

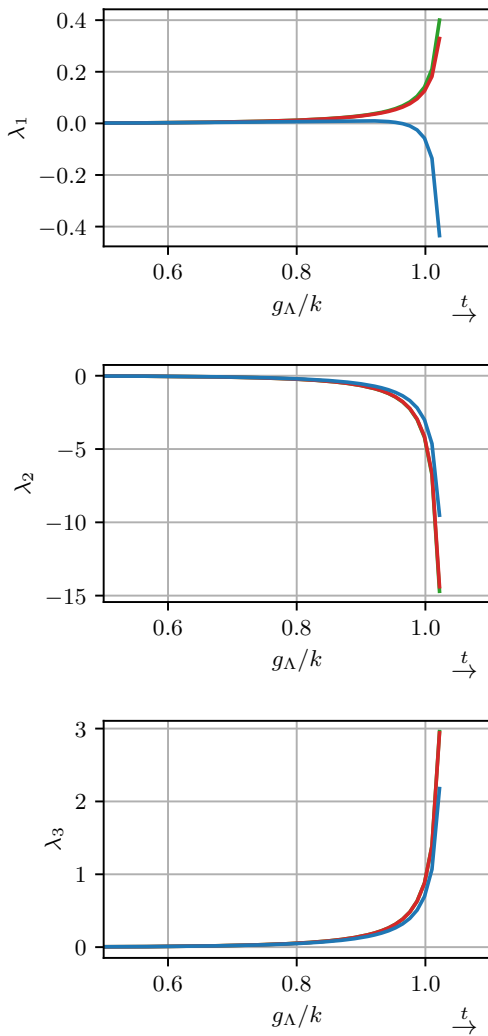


FIG. 7. The numerical solution to the flow equations of the four-fermion couplings is depicted with $m_\Lambda/g_\Lambda = 10^{-2}$ and $\lambda_i = 0$ at scale $\Lambda/g_\Lambda = 10^5$ and $N_c = 3$. Contributions from the box-diagrams in Fig. 4 only are shown in blue, adding those from the triangle-diagrams from Fig. 5 in red and again adding the purely fermionic diagrams from Fig. 6 in green.

tions of the gauge coupling and fermion mass, Eqs. (59) and (60), we have to make use of numerical integration. The UV-limit helps to test the numerical implementation against an analytical solution. The numerical results are shown in Fig. 7 where we distinguish between the contribution from all diagrams, the box-diagrams plus triangle-diagrams, and the box-diagrams only. We find that all couplings are driven to $\pm\infty$ by the gauge coupling that develops its singularity. The box-diagrams (two gluon exchange diagrams) are the most important in the UV regime because they generate the couplings and dominate the flows as long as their values are small compared to \tilde{g} . The triangle-diagrams become more relevant at scales $k/g_\Lambda \simeq 1$ and leads to a stronger growth of the couplings. Their impact is crucial for the coupling λ_1 .

There is a sign change in the flow which seems to be a special feature for $N_c = 3$. Knowledge about the sign is important to the flow equations of the purely fermionic diagrams. At this point, it is not clear yet how much they are of importance during the flow. Their contribution is barely visible, but integrating towards even lower scales becomes problematic where we expect our truncation to break down.

3. Limit of zero gauge coupling

Let us also consider the limit of vanishing gauge coupling, $g \rightarrow 0$, which reduces the model to a purely four-fermion theory in 1 + 1 dimensions. This is of interest for several (related) reasons:

1. The purely fermionic model alone is of interest as a standalone QFT. It treats a Fierz-complete set of four-fermion interactions and one can learn, amongst other things, about the validity of a one or few channel approximation like the GN model.
2. The divergence in the gauge coupling prevents us from gaining insights in the dynamics caused by the purely fermionic diagrams shown in Fig. 6. The simplest way to study these contributions is to manually “switch off” the gauge sector by setting $g = 0$. Another approach, which we do not follow within this work, would be to artificially regularize the gauge sector in a way that renders the flow of the gauge coupling finite and nonzero in the IR.
3. The limit corresponds to a scenario where the purely fermionic diagrams are the dominant ones. This may indeed be the case for a more sophisticated truncation of the effective action in its gauge sector that renders the flow of the dimensionless gauge coupling finite. In four dimensions, this has been achieved [114] and we expect a similar behaviour for two dimensions.

Hence, the flow equations that we consider in the following are,

$$\partial_t \lambda_1 = \frac{(\lambda_1)^2 N_c - (\lambda_1 + \lambda_2)(\lambda_1 + 2\lambda_3)}{\pi N_c (1 + \tilde{m})}, \quad (103)$$

$$\partial_t \lambda_2 = -\frac{(\lambda_2)^2 N_c - (\lambda_1 + \lambda_2)(\lambda_2 - 2\lambda_3)}{\pi N_c (1 + \tilde{m})}, \quad (104)$$

$$\partial_t \lambda_3 = -\frac{\lambda_1 \lambda_2}{\pi N_c (1 + \tilde{m})}. \quad (105)$$

For a derivation, see Ref. [30, App. I]. Here, we assume a vanishing anomalous dimension which we justify in Section VI F. Furthermore, we do not include the flow of the fermion mass. Its flow is in fact not UV-finite which we elaborate on in Section VI F. Anyways, the mass is not

very important in the present discussion because it only appears in a global pre-factor and can be absorbed by a redefinition of the RG time and RG scale.

Inspecting Eqs. (103) to (105), we recognize the flow equation of the two-dimensional GN model in the limit $\lambda_2 = \lambda_3 = 0$. We also find that the flow equation of λ_3 is a bit special because there is no $(\lambda_3)^2$ term. It is presumably a coincidence for the particular regularization scheme and spacetime dimension as pointed out below in Section VI E.

The key feature in two dimensions is, that there is no term linear in the couplings in the flow equations that would stem from rescaling the couplings to dimensionless quantities. As expected from the Fierz complete ansatz, there are terms that couple the equations nonlinearly. However, if there is only one of the couplings that is nonzero, it does not generate the other couplings and working with one channel is exact. Another remarkable observation is that if $\lambda_1 = -\lambda_2$ is satisfied at some scale, it holds at all scales. Hence, even though the regulator insertion does not respect chiral symmetry, it can be restored in the flow of the four-fermion couplings, see also Eq. (94). We conclude that, in the full setup, the gluon exchange diagrams are actually responsible for the breaking of the chiral symmetry with the fermionic regulator.

The couplings must be initialized at nonzero values to obtain a nontrivial flow. The case $\lambda_1 = \lambda_2 = \lambda_3 = 0$ corresponds to a Gaussian fixed point, if there are no gluons present. The class of values where $\lambda_1 = \lambda_2 = 0$ contains the only fixed points of the model. It has an attractive direction which is exemplary shown in Fig. 8 and derived in greater detail in Ref. [30, Sec. 5.3.3]. However, starting from initial conditions, where the couplings approach a fixed point in the IR, one can show that the couplings diverge for an integration towards the UV. This behavior is known in the GN model as well. In contrast, the mutual coupling of the flow equations in the present case allows for some couplings to be initially driven away from the fixed point that is ultimately reached.

The other scenario is that the couplings diverge at a certain scale. They approach $\pm\infty$. This is also known from the GN and related models. Here, however, the mutual coupling of the equations makes it intricate to determine the precise parameter space for this or the fixed point scenario. Two examples are shown in Figs. 9 and 10. The example in Fig. 10 illustrates once more that very large RG times must sometimes be resolved.

The interesting question is of course whether the gauge dynamics drive the couplings to values which either diverge or approach a fixed point due to the purely fermionic dynamics. The observation is that the case of the divergence is relevant to QCD₂. It seems that the fixed point scenario requires specially balanced coupling values while the divergence is more generic in the Fierz-complete model as the divergence is close to the underlying properties of the GN-type model.

The growing fermionic self-interactions ending up in

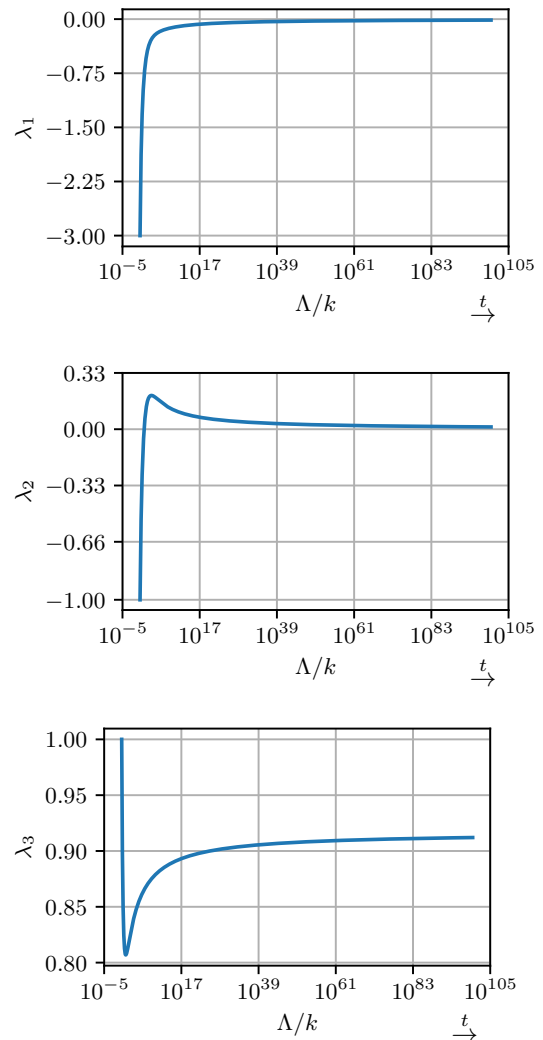


FIG. 8. Flow of the four-fermion couplings into a fixed point in purely fermionic dynamics. At $t = 0$ the values are $\lambda_i = (-3.0, -1.0, 1.0)$.

a singularity have an important physical significance. It signals the possible formation of condensates and mesonic bound states/resonances. This can be best understood by means of a Hubbard–Stratonovich transformation [115, 116], where one treats the quark bilinears as auxiliary bosonic fields coupled to the quarks via a Yukawa interaction. This method is well-known in condensed matter and high energy physics, see, *e.g.*, Ref. [117] for a review. What is important is that the four-fermion couplings are inversely proportional to the mass of the bosonic field. If it approaches its singularity, mesonic particles are produced with very little energy and, eventually, it signals the formation of a condensate. The fermionic interactions can no longer be approximated as being local. Instead, momentum dependence must be resolved for example by methods of partial bosonization, which is further outlined in the outlook, Section VII. In other words, bound states form during the flow but their

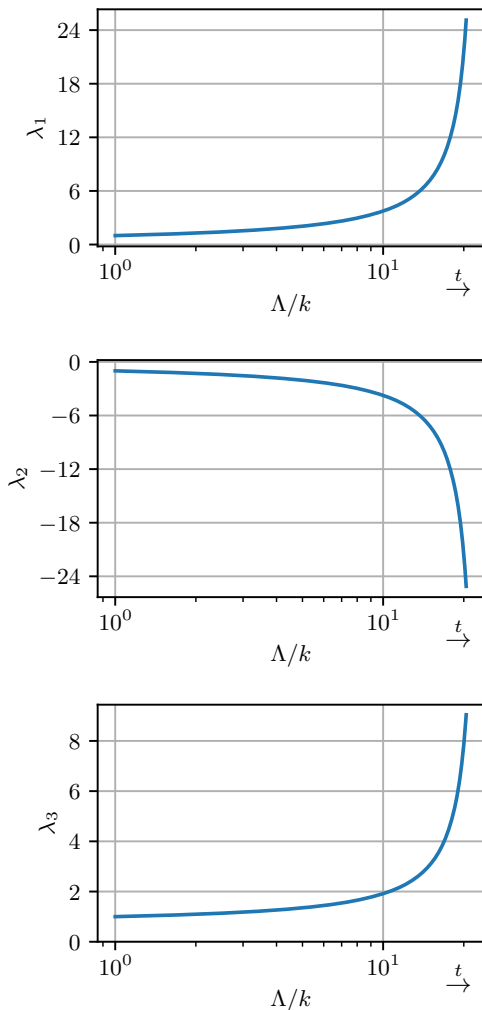


FIG. 9. Flow of the four-fermion couplings in purely fermionic dynamics. At $t=0$ initial conditions $\lambda_i(k=\Lambda) = (-1.0, -1.0, 1.0)$ are chosen.

mass decreases for increasing four-fermion coupling making their propagation non-negligible. Hence, one might argue that the divergence of the four-fermion couplings already signals the limitations of the approximation and range of validity and suggests the path to a more sophisticated truncation.

We recap this investigation with focus on the relevance of the dimension $d=2$ and the Fierz completeness of our ansatz. The purely fermionic dynamics lead to either a divergence of the four-fermion couplings or to a fixed point where most couplings become zero. The former case seems to be the relevant scenario for QCD_2 . In two dimensions, there is no critical absolute value to which the couplings must be driven to enter this scenario, which is different from $3+1$ dimensional QCD.

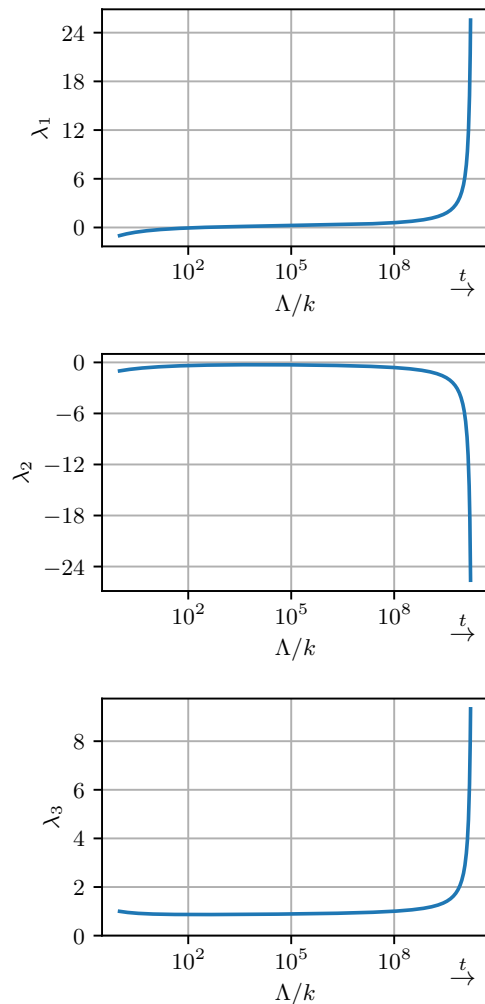


FIG. 10. Flow of the four-fermion couplings in purely fermionic dynamics. At $t=0$ initial conditions $\lambda_i(k=\Lambda) = (-1.0, -1.0, 1.0)$ are chosen.

4. Infinite- N_c limit

Another interesting limit is the infinite- N_c limit as already motivated and discussed for the minimal ansatz in Section V E 3. In addition, many models are exactly solvable in this limit and different questions can be addressed analytically. For instance, the 't Hooft solution [5] reveals the bound states of the theory while the GN model can be solved to obtain even its phase diagram [110, 118], see Refs. [93, 119, 120] for more examples.

There is no further rescaling of the couplings $\lambda_1, \dots, \lambda_3$ necessary because there is already a factor $1/N_c$ included in the definition in Eq. (89). On a diagrammatic level, the two top diagrams in Figs. 4 and 5 as well as the right one in Fig. 6 are suppressed in this limit. As we will see, the contributions from the remaining diagrams also simplify significantly. For explicit expressions for the equations we refer to Ref. [30, App. I].

We find that the flow of the third channel vanishes

completely in this limit. This is presumably a regulator feature in combination with the spacetime dimension $d = 2$ as will be discussed in Section VI E.

The major observation, however, is that the flow equations decouple such that the flow of λ_i does exclusively depend on the gauge coupling, the fermion mass and the coupling λ_i itself. We emphasize that this holds on all scales and it is a feature of the chosen basis of interactions. Not only does this happen because the mentioned diagrams drop out, but also the remaining diagrams simplify. Similar observation have been made in Ref. [100] for the $(3 + 1)$ -dimensional case.

There is no analytical solution to the full system of flow equations because of the mass term. The purely fermionic diagrams, however, simplify to the GN equations which is investigated in detail in Appendix E. The GN equations admit an exact solution, see *e. g.*, Ref. [69, Sec. 9].

The conclusion is that it would be possible to work in a non Fierz-complete basis in this limit because the equations decouple.

E. Regulator dependences

This section summarizes a few consistency checks that have been carried out using a different regulator for the fermions, namely the Litim regulator [75],

$$\Delta S_k = \int_q \bar{\psi}(-q) \not{q} r_f(q) \psi(q), \quad (106)$$

where the Litim regulator shape function is given by

$$r_f(q) \equiv \left(\sqrt{\frac{k^2}{q^2} - 1} \right) \Theta \left(\frac{k^2}{q^2} - 1 \right), \quad (107)$$

where Θ is the Heaviside step function.

It has major deficiencies compared to the momentum-independent regulator (33), which is why it was not chosen in this work. First of all, the momentum dependence destroys gauge invariance. Only covariant derivatives should appear. Moreover, it introduces crucial nonanalyticities at vanishing momentum and ruins spectral properties. Unitarity is broken or the Osterwalder–Schrader reflection positivity is violated in the Euclidean domain. On the other hand, the Litim regulator preserves axial symmetry, because it is proportional to γ^μ , which is a significant advantage and can be used for some consistency checks.

Repeating the calculations with this regulator, we confirm that axial symmetry is indeed preserved: setting the bare quark mass to zero, its flow vanishes and one indeed has $\partial_t(\lambda_1 + \lambda_2) = 0$ from all types of diagrams if $\lambda_1 = -\lambda_2$ holds at a particular scale, *e.g.* in the UV.

It is possible to draw a few more conclusions. The flow of the four-fermion couplings also decouples with this regulator in the infinite- N_c limit suggesting that this is not

a unique feature of the local regulator. Moreover, the contributions from the box- and triangle-diagrams to the flow of the coupling λ_3 also vanish in this limit. But there is a contribution from the purely fermionic diagrams in Fig. 6, which is a term proportional to $(m/k)\lambda_3^2$. Therefore, one has to be careful about drawing strong conclusions from the simplification of the flow equation of λ_3 , Eq. (105).

However, a detailed analysis of using other regulators is beyond the scope of this work and might be subject to future investigations. Moreover, we highlight again the importance of property 1 that is obeyed by the local regulator and why we focus on it in this work.

F. Contribution to quark two-point vertex

So far, it was neglected that the four-fermion couplings also drive the flow of the full fermion two-point vertex function. Equation (46) therefore obtains a new term which is of “tadpole”-type,

$$\partial_t \text{---} \circ \text{---} = \text{---} \circ \text{---} + \text{---} \circ \text{---} + \text{---} \circ \text{---} . \quad (108)$$

The first diagram is independent of the external momentum meaning that there is no contribution to the anomalous dimension because a projection onto the kinetic term consists of taking a derivative w.r.t. the external momentum yielding zero. As already mentioned in Section V D, a vanishing anomalous dimension η_ψ implies that the projection of the r.h.s. of the Wetterich equation onto the fermion-gluon vertex must give zero. However, the four-fermion vertex allows for an additional diagram, which was not present before,

$$\partial_t \text{---} \circ \text{---} = \text{---} \circ \text{---} . \quad (109)$$

We verified explicitly that its projection gives no contribution. However, Eq. (108) gives a new contribution to the flow of the fermion mass. Because the four-fermion couplings are dimensionless and we use a mass-like regulator, the diagram is logarithmically UV-divergent. Even though the couplings are initialized at zero, fluctuations always contribute on all scales with a mass-like regulator. Formulae on the divergence and how the diagram can be regularized by an additional Pauli–Villars regularization are given in Ref. [30, Sec. 5.5].

A solution to this problem might be to resolve the momentum dependence of the four-fermion couplings, which is expected to suppress the large-momentum contributions in the loop. Consequently, the problem certainly arises because of our (a bit too) simplistic truncation. The diagrams in Figs. 4 to 6 of course carry a momentum dependence. It is partly worked out in Ref. [30, Sec. G.3] and we anyway have to resolve it to deal with the divergence of the four-fermion couplings. We discuss these upcoming steps of our research program in the following outlook.

VII. OUTLOOK: BOSONIZATION

The next step for improving the truncation in the matter sector is to resolve the momentum dependence of the four-fermion couplings. It is the key to understanding the IR physics of the model and to accessing the formation of (mesonic) bound states. This can be pursued either on the level of the four-fermion couplings themselves, as done in Refs. [102, 103] in four dimensions with certain approximations, or by means of a “flowing bosonization”. This technique maps the nonlocalities of the four-fermion vertices to a local description in terms of a Yukawa coupling and meson exchanges [59]. Diagrammatically speaking this means

$$(110)$$

where the dots stand for those parts of the momentum dependent vertex which cannot be written in terms of meson exchanges (dotted double lines) and a Yukawa coupling. The Yukawa coupling will be of positive energy dimension and the “tadpole”-type contribution to the fermion two-point vertex in Eq. (108) will be replaced by self-energy diagrams as in Eq. (46), but with meson instead of gluon lines. This will lead to UV-finiteness in all flow equations.

A challenge is that this formulation cannot be achieved by a one-off Hubbard–Stratonovich transformation, but it must be implemented continuously at all RG-scales for which Refs. [121–123] provide a recipe. A great advantage of working in two dimensions compared to four is that there are much less possible bound states. Hence, we aim to bosonize each channel in future work.

At the same time, we plan to improve the truncation in the gauge sector to remove the divergence of

the gauge coupling, at least, to significantly lower scales than where the four-fermion couplings diverge due to the purely fermionic dynamics.

VIII. SUMMARY AND CONCLUSION

In summary, we have studied QCD with massive quarks in the fundamental representation of the gauge group, in $d = 2$ spacetime dimensions. Our starting point was the Euclidean functional integral and generating functionals for quarks and gauge fields, as well as ghosts after gauge fixing. The latter was done using the background field variant of covariant gauges (and we concentrated on Feynman–’t Hooft gauge for the numerical part of our calculations).

In a subsequent step we introduced a mass-like IR regularization for all fluctuating fields. When the corresponding regulator scale is very large, quantum fluctuations are suppressed, while they get included successively when the regularization scale is lowered. We carefully examined how the presence of the IR regularization modifies generating functionals, and in particular identities related to gauge invariance they obey: Ward–Takahashi, Slavnov–Taylor, and Nielsen. Because UV divergences are very mild in $d = 2$ dimensions, we can work with a momentum-independent regulator that preserves the Ward–Takahashi identity in an unmodified way, and the Nielsen identity also has no explicit regulator dependence. BRST symmetry is broken, and the Slavnov–Taylor identity is accordingly modified, however.

As a super-renormalizable theory, QCD₂ is well controlled in the UV regime. The gauge coupling, which has dimensions of energy, goes to a fixed value and a UV regularization can be removed. The IR, on the other side, is more problematic. To get started, we made a relatively simple ansatz, or truncation, for the flowing quantum effective action with only two flowing parameters, the gauge coupling and the fermion mass. The wavefunction renormalization factor for quarks turned out not to flow within the truncation and gauge fixing we have chosen.

Being close to the perturbative framework, our truncation allowed to reproduce the perturbative one-loop result for the beta functions, but also already contains non-perturbative elements beyond that. In the IR regime, we find that the gauge coupling and, as a consequence, also the fermion mass diverge. One should be careful in drawing too many conclusions from this finding because the flow equations for QCD in $d = 4$ dimensions would likely behave similar for a truncation as simple as ours. Further investigations are needed before definite conclusions can be drawn concerning the IR sector.

One obvious question concerns the dependence on the gauge fixing. Besides Feynman–’t Hooft gauge it would be useful to study other covariant gauges in future work. We are also planning to explore light-cone gauge further, especially to connect more directly to the pioneering work of ’t Hooft.

Within our present approximation, it was also interesting to vary the gauge group through the number of color charges N_c , and the number of quark flavors N_f . When lowering the ratio of the number of gauge bosons to fermions below a certain threshold, we found that there is a window in the RG flow, where the gauge coupling first decreases, before it ultimately also diverges towards the IR for massive quarks. Only for an infinite number of fermionic flavors it is possible to fully integrate the flow to the IR and to fully remove the regulator in our current truncation, and to arrive in a weakly coupled regime.

Going beyond gauge field dynamics, we also investigated local fermion-fermion interaction terms of various kinds. These are generated by the RG flow from gluon and quark field fluctuations. This basic mechanism is well known from QCD in $d = 4$ dimensions and still works in $d = 2$ despite the fact that there are no propagating gluons.

Via two different approaches, (1.) expansion in the full tensor structure and (2.) projection and algebraically solving for the RG flows of the single couplings, we explained and worked out that there are only three algebraically independent local fermion interaction terms in the case of one flavor, $N_f = 1$. Chiral symmetry for massless quarks would reduce this further to two. We also included the feedback of these local fermion interaction couplings to the flow, once they have been generated. Also within this extended truncation there is still the IR divergence stemming from the gauge coupling at which the flow breaks down.

We observed that the fermion-gluon dynamics drive the four-fermion couplings to large values and ultimately to a divergence. This divergence is not necessarily due to the divergence of the gauge coupling. It can also occur in purely fermionic theories with frozen or vanishing gauge coupling once the fermion-fermion couplings are nonzero. Divergent local four-fermion couplings should be interpreted as a first signal for the formation of bound states and the relevance of the respective interaction channels – at least at intermediate RG scales. We remark that, even though chiral symmetry is broken by the fermionic part of the Callan–Symanzik regulator, the RG flow of the four-fermion couplings produces the correct signs of the couplings that would be required for full chiral symmetry.

In upcoming work, we plan to better resolve the frequency and momentum dependence of quark interaction vertices and especially to resolve the branch cuts and poles related to resonances and bound states. The precise determination of the spectrum of bound states and resonances through the RG flow is the most important motivation and future goal for us.

ACKNOWLEDGEMENTS

We thank Holger Gies for useful discussions and Markus Huber for support with the DOFUN software-

package. S.F. thanks Moaathe Belhaj Ahmed for collaboration on related work and E.O. acknowledges support from the Stiftung der Deutschen Wirtschaft (sdw).

Appendix A: BRST symmetry

Here, we formulate the BRST-symmetry [60, 61] within the background-field method similar to Ref. [124, Sec. 3.2.1], see also Ref. [52, Sec. 16.4] for the case without a background-field. To do so, we introduce non-dynamical, auxiliary fields B^z , $z \in \{1, \dots, N_c^2 - 1\}$, oftentimes denoted as Nakanishi-Lautrup fields [125, 126],

$$\begin{aligned} S[\bar{\psi}, \psi, a, \bar{A}, \bar{c}, c] & \quad (A1) \\ &= \int_x \left[\bar{\psi} (\gamma^\mu D_\mu + m) \psi + \frac{1}{2g^2} \text{tr}(F_{\mu\nu} F^{\mu\nu}) \right. \\ & \quad \left. - \bar{c} D^\mu [\bar{A}] D_\mu [a + \bar{A}] c + \frac{\xi}{2} B^2 + \frac{1}{g} B D^\mu [\bar{A}] a_\mu \right], \end{aligned}$$

over which we also integrate in the path integral. Hence, Eqs. (19) and (A1) are equivalent because B can simply be integrated out. A global BRST transformation with infinitesimal parameter ϵ is given by

$$\bar{A}_\mu^z \mapsto \bar{A}'_\mu{}^z = \bar{A}_\mu^z + 0, \quad (A2)$$

$$a_\mu^z \mapsto a'^\mu{}_z = a_\mu^z + \epsilon D_\mu [a + \bar{A}]^z{}_w c^w, \quad (A3)$$

$$\psi \mapsto \psi' = \psi + i \epsilon c^z T_z \psi, \quad (A4)$$

$$\bar{\psi} \mapsto \bar{\psi}' = \bar{\psi} - i \epsilon \bar{\psi} c^z T_z, \quad (A5)$$

$$c^z \mapsto c'^z = c^z - \frac{1}{2} \epsilon f^z{}_{uv} c^u c^v, \quad (A6)$$

$$\bar{c}^z \mapsto \bar{c}'^z = \bar{c}^z + \epsilon B^z, \quad (A7)$$

$$B^z \mapsto B'^z = B^z + 0. \quad (A8)$$

The fluctuation-field a carries the BRST transformation in these formulas. It is not the only possible way of distributing the BRST transformation over the fields [124, Sec. 3.2.1]. The BRST-invariance is of importance because it must also be present in the quantum effective action.

Appendix B: Ward identity for CS-type regulators

In presence of an arbitrary regulator piece, the Ward–Takahashi identity (28) becomes the *modified Ward–Takahashi identity* for Γ_k [59, Eq. (74)],

$$\mathcal{G}^z(\Gamma_k + \Delta S_k) = \langle \mathcal{G}^z(S_{\text{gf}} + S_{\text{gh}} + \Delta S_k) \rangle_{J[\Phi]}. \quad (B1)$$

Recall that Γ_k is not yet evaluated at $\bar{A} = A$ and $a = 0$. The regulator based modification, $(\mathcal{G}^z \Delta S_k) - \mathcal{G}^z \Delta S_k$, vanishes for the local regulator (33). We partly follow Ref. [59, Sec. 3.4] to prove this. The quark and ghost parts are individually invariant under gauge transformations. Focusing on the gauge field only and using Eq. (29), we calculate

$$\begin{aligned} D_\mu [a + \bar{A}]^z_w \frac{\delta}{\delta a_{\mu w}(x)} \int_y \frac{k^2}{g^2} \text{tr}[a_\mu(y) a^\mu(y)] \quad (\text{B2}) \\ = \frac{k^2}{g^2} \left(\delta_w^z \partial_\mu + f^z_{uw} [a_\mu^u(x) + \bar{A}_\mu^u(x)] \right) a^{\mu w}(x) \\ = \frac{k^2}{g^2} [\partial_\mu a^{\mu z}(x) + f^z_{uw} \bar{A}_\mu^u(x) a^{\mu w}(x)]. \end{aligned}$$

The final expression is linear in the fluctuation-field which implies that both regulator terms in Eq. (B1) automatically cancel. The key property of the Callan–Symanzik-type regulator that leads to this result is that it is diagonal in color space.

Appendix C: Derivation of the modified Nielsen identity

We derive Eq. (37) and a more general result for arbitrary regulator pieces using the field space vectors

$$\Phi_{\mathbf{a}} = (\psi, \bar{\psi}, a, c, \bar{c})_{\mathbf{a}}, \quad (\text{C1})$$

$$\bar{\Phi}_{\mathbf{a}} = (\psi, \bar{\psi}, a + \bar{A}, c, \bar{c})_{\mathbf{a}}, \quad (\text{C2})$$

$$J^{\mathbf{a}} = (\bar{\eta}, -\eta, J, \bar{\omega}, -\omega)_{\mathbf{a}}. \quad (\text{C3})$$

As an auxiliary calculation, we need the functional derivative of the Schwinger functional w.r.t. the background field at fixed source,

$$\begin{aligned} \frac{\delta W_k}{\delta \bar{A}} \Big|_J &= \quad (\text{C4}) \\ &= \frac{1}{Z_k} \int \mathcal{D}\Phi \frac{\delta}{\delta \bar{A}} e^{-(S_{\text{QCD}_2} + S_{\text{gf}} + S_{\text{gh}}) + J^{\mathbf{a}} \bar{\Phi}_{\mathbf{a}} - \Delta S_k} \\ &= \frac{1}{Z_k} \int \mathcal{D}\Phi e^{-(S_{\text{gf}} + S_{\text{gh}} + \Delta S_k)} \frac{\delta}{\delta \bar{A}} \left(e^{-S_{\text{QCD}_2} + J^{\mathbf{a}} \bar{\Phi}_{\mathbf{a}}} \right) \\ &\quad - \left\langle \frac{\delta(S_{\text{gf}} + S_{\text{gh}})}{\delta \bar{A}} \right\rangle \\ &\quad - \frac{1}{Z_k} \int \mathcal{D}\Phi \frac{\delta \Delta S_k}{\delta \bar{A}} e^{-(S_{\text{QCD}_2} + S_{\text{gf}} + S_{\text{gh}}) + J^{\mathbf{a}} \bar{\Phi}_{\mathbf{a}} - \Delta S_k} \\ &= \frac{1}{Z_k} \int \mathcal{D}\Phi e^{-(S_{\text{gf}} + S_{\text{gh}} + \Delta S_k)} \frac{\delta}{\delta a} \left(e^{-S_{\text{QCD}_2} + J^{\mathbf{a}} \bar{\Phi}_{\mathbf{a}}} \right) \end{aligned}$$

$$\begin{aligned} &- \left\langle \frac{\delta(S_{\text{gf}} + S_{\text{gh}})}{\delta \bar{A}} \right\rangle - \frac{1}{2} \left[\text{STr} \left(\frac{\delta R_k}{\delta \bar{A}} G_k \right) + \Phi \frac{\delta R_k}{\delta \bar{A}} \Phi \right] \\ &= \frac{1}{Z_k} \int \mathcal{D}\Phi \frac{\delta}{\delta a} \left(e^{-(S_{\text{QCD}_2} + S_{\text{gf}} + S_{\text{gh}} + \Delta S_k) + J^{\mathbf{a}} \bar{\Phi}_{\mathbf{a}}} \right) \\ &\quad + \left\langle \frac{\delta(S_{\text{gf}} + S_{\text{gh}})}{\delta a} \right\rangle + \frac{\delta \Delta S_k}{\delta a} - \left\langle \frac{\delta(S_{\text{gf}} + S_{\text{gh}})}{\delta \bar{A}} \right\rangle \\ &\quad - \frac{1}{2} \text{STr} \left(\frac{\delta R_k}{\delta \bar{A}} G_k \right) - \frac{1}{2} \Phi \frac{\delta R_k}{\delta \bar{A}} \Phi \\ &= \left\langle \frac{\delta(S_{\text{gf}} + S_{\text{gh}})}{\delta a} - \frac{\delta(S_{\text{gf}} + S_{\text{gh}})}{\delta \bar{A}} \right\rangle + \frac{\delta \Delta S_k}{\delta a} \\ &\quad - \frac{1}{2} \text{STr} \left(\frac{\delta R_k}{\delta \bar{A}} G_k \right) - \frac{\delta \Delta S_k}{\delta \bar{A}}. \end{aligned}$$

Using this result, we obtain

$$\begin{aligned} \frac{\delta \Gamma_k}{\delta \bar{A}} \quad (\text{C5}) \\ &= \int_x \left(\frac{\delta J^{\mathbf{a}}}{\delta \bar{A}} \bar{\Phi}_{\mathbf{a}} + J^{\mathbf{a}} \frac{\delta \bar{\Phi}_{\mathbf{a}}}{\delta \bar{A}} \right) - \frac{\delta J^{\mathbf{a}}}{\delta \bar{A}} \frac{\delta W_k}{\delta J^{\mathbf{a}}} \\ &\quad - \frac{\delta W_k}{\delta \bar{A}} \Big|_J - \frac{\delta \Delta S_k}{\delta \bar{A}} \stackrel{(\text{C4})}{=} \\ &= \frac{\delta \Gamma_k}{\delta a} + \frac{\delta \Delta S_k}{\delta a} - \left\langle \frac{\delta(S_{\text{gf}} + S_{\text{gh}})}{\delta a} - \frac{\delta(S_{\text{gf}} + S_{\text{gh}})}{\delta \bar{A}} \right\rangle \\ &\quad - \frac{\delta \Delta S_k}{\delta a} + \text{STr} \left(\frac{\delta R_k}{\delta \bar{A}} G_k \right). \end{aligned}$$

Re-arranging the terms yields the result

$$\begin{aligned} \frac{\delta \Gamma_k}{\delta \bar{A}} - \frac{\delta \Gamma_k}{\delta a} + \left\langle \frac{\delta(S_{\text{gf}} + S_{\text{gh}})}{\delta a} - \frac{\delta(S_{\text{gf}} + S_{\text{gh}})}{\delta \bar{A}} \right\rangle \\ = \frac{1}{2} \text{STr} \left(\frac{\delta R_k}{\delta \bar{A}} G_k \right). \quad (\text{C6}) \end{aligned}$$

On-shell evaluation with sources

$$J^{\mathbf{a}} = \frac{\delta \Delta S_k[\Phi]}{\delta \bar{\Phi}_{\mathbf{a}}} \quad (\text{C7})$$

leads to $\delta \Gamma_k / \delta a = 0$ and a vanishing of the expectation value on the l.h.s. of Eq. (C6),

$$\begin{aligned} \left\langle \frac{\delta(S_{\text{gf}} + S_{\text{gh}})}{\delta a} - \frac{\delta(S_{\text{gf}} + S_{\text{gh}})}{\delta \bar{A}} \right\rangle_{J = \frac{\delta \Delta S_k}{\delta \bar{\Phi}}} \quad (\text{C8}) \\ = \frac{1}{Z_k} \int \mathcal{D}\Phi \left(\frac{\delta}{\delta \bar{A}} - \frac{\delta}{\delta a} \right) e^{-(S_{\text{QCD}_2} + S_{\text{gf}} + S_{\text{gh}})} \\ = \frac{1}{Z_k} \frac{\delta}{\delta \bar{A}} \int \mathcal{D}\Phi e^{-(S_{\text{QCD}_2} + S_{\text{gf}} + S_{\text{gh}})} = 0. \end{aligned}$$

The last line is zero for the reason which is referred to as “the Faddeev–Popov trick can be undone” in Ref. [53, Sec. 5.2.1]. The on-shell modified Nielsen identity therefore reads

$$\frac{\delta \Gamma_k}{\delta A} = \frac{1}{2} \text{STr} \left(\frac{\delta R_k}{\delta A} G_k \right). \quad (\text{C9})$$

The r.h.s. is zero for vanishing cutoff, *c.f.* Eq. (32), or the local regulator, *c.f.* Eq. (37).

Appendix D: Rescaling of the gauge field

There are two ways of introducing renormalized quantities in the gauge sector. For the first one the starting point is the bare action

$$S = \frac{1}{2} \int \text{tr}(F_{\text{bare}}^{\mu\nu} F_{\text{bare},\mu\nu}) \quad (\text{D1})$$

where the field strength is built from the covariant derivative

$$D_\mu = \partial_\mu - i g_{\text{bare}} A_{\text{bare},\mu}. \quad (\text{D2})$$

Next, introduce a scale-dependent wave function renormalization

$$S = \frac{Z_k}{2} \int \text{tr}(F_{\text{bare}}^{\mu\nu} F_{\text{bare},\mu\nu}). \quad (\text{D3})$$

Absorb it into the field

$$\bar{A}_\mu = \sqrt{Z_k} A_{\text{bare},\mu}, \quad (\text{D4})$$

$$S = \frac{1}{2} \int \text{tr}(\bar{F}^{\mu\nu} \bar{F}_{\mu\nu}), \quad (\text{D5})$$

$$D_\mu = \partial_\mu - i \frac{g_{\text{bare}}}{\sqrt{Z_k}} \bar{A}_\mu. \quad (\text{D6})$$

Redefine the coupling to g_k such that

$$D_\mu = \partial_\mu - i g_k \bar{A}_\mu, \quad (\text{D7})$$

$$0 = \partial_k (g_k \sqrt{Z_k}), \quad (\text{D8})$$

and absorb it into the field

$$S = \frac{1}{2g_k^2} \int \text{tr}(F^{\mu\nu} F_{\mu\nu}). \quad (\text{D9})$$

Putting all steps together, one has not rescaled with a scale-dependent quantity, but just with g_{bare} . The two terms in the flow equation cancel due to Eq. (D8). Because of that identity there is in fact just one independent renormalization parameter.

The starting point of the second approach is again the bare action

$$S = \frac{1}{2} \int \text{tr}(F_{\text{bare}}^{\mu\nu} F_{\text{bare},\mu\nu}). \quad (\text{D10})$$

One immediately absorbs the coupling in the gauge fields to remove the coupling from the gauge-covariant derivative,

$$S = \frac{1}{2g_{\text{bare}}^2} \int \text{tr}(F^{\mu\nu} F_{\mu\nu}), \quad (\text{D11})$$

$$D_\mu = \partial_\mu - i A_\mu. \quad (\text{D12})$$

Next, we allow the gauge coupling to be scale-dependent

$$S = \frac{1}{2g_k^2} \int \text{tr}(F^{\mu\nu} F_{\mu\nu}). \quad (\text{D13})$$

Here, however, there is no additional need to introduce a Z_k . Still, one has to introduce this term for the matter sector. In any case, the two approaches are equivalent and both keep the structure of the gauge-covariant derivative intact.

Appendix E: Infinite- N_c limit of four-fermion flow equations

We investigate the purely fermionic dynamics in more detail. In particular, we explain why the corresponding flow equations for the four-fermion couplings decouple in the infinite- N_c limit for the specific choice of the Fierz-complete basis.

The first step towards this goal does not make use of these specifications yet. We re-derive the flow equations for the four-fermion couplings in an arbitrary number of spacetime dimensions for a general basis $\{\mathcal{O}_i\}$ of matrices such that $\{(\bar{\psi} \mathcal{O}_i \psi)^2\}$ is Fierz-complete. Therefore, we utilize the background-field method applied to the fermionic field: we split it into a background-field $\psi, \bar{\psi}$ and a fluctuation field $\psi', \bar{\psi}'$ and extract from the four-fermion interaction the term bilinear in the fluctuation fields,

$$\begin{aligned} & [(\bar{\psi} + \bar{\psi}') \mathcal{O}_i (\psi + \psi')]^2 \quad (\text{E1}) \\ &= [\bar{\psi} \mathcal{O}_i \psi + \bar{\psi} \mathcal{O}_i \psi' + \bar{\psi}' \mathcal{O}_i \psi + \bar{\psi}' \mathcal{O}_i \psi']^2 \\ &= 2(\bar{\psi} \mathcal{O}_i \psi)(\bar{\psi}' \mathcal{O}_i \psi') + 2(\bar{\psi} \mathcal{O}_i \psi')(\bar{\psi}' \mathcal{O}_i \psi) + \dots \end{aligned}$$

We proceed with the Wetterich equation in its log-form and expand its r.h.s. up to quartic order in the fermionic field to project on the flow of the four-fermion couplings. Denoting the free-part of $(\Gamma_k^{(2)} + \Delta S_k)$ by P , we obtain (summation over i, j is implied)

$$\begin{aligned} & (\partial_t \lambda_i + 2\eta_\psi \lambda_i) (\bar{\psi} \mathcal{O}_i \psi) (\bar{\psi} \mathcal{O}_i \psi) \quad (\text{E2}) \\ &= \text{STr} \left[\tilde{\partial}_t \left([\lambda_i (\bar{\psi} \mathcal{O}_i \psi) \mathcal{O}_i + \lambda_i \mathcal{O}_i \psi \bar{\psi} \mathcal{O}_i] P^{-1} \right) \right] \end{aligned}$$

$$\begin{aligned}
& \times [\lambda_j (\bar{\psi} \mathcal{O}_j \psi) \mathcal{O}_j + \lambda_j \mathcal{O}_j \psi \bar{\psi} \mathcal{O}_j] P^{-1} \Big) \Big] \\
& = \lambda_i \lambda_j \left[(\bar{\psi} \mathcal{O}_i \psi) (\bar{\psi} \mathcal{O}_j \psi) \text{STr}(\tilde{\partial}_t [P^{-1} \mathcal{O}_i P^{-1} \mathcal{O}_j]) \right. \\
& \quad + 2 (\bar{\psi} \mathcal{O}_i \psi) \text{STr}(\tilde{\partial}_t [P^{-1} \mathcal{O}_i P^{-1} (\mathcal{O}_j \psi \bar{\psi} \mathcal{O}_j)]) \\
& \quad \left. + \text{STr}(\tilde{\partial}_t [P^{-1} (\mathcal{O}_i \psi \bar{\psi} \mathcal{O}_i) P^{-1} (\mathcal{O}_j \psi \bar{\psi} \mathcal{O}_j)]) \right].
\end{aligned}$$

The first term is already in the desired form of l.h.s. such that one can read off the flow equations by comparing both sides. The other terms are not of this form yet. In general, one would have to expand the matrix structure connecting $\bar{\psi}$ with ψ in terms of the basis $\{\mathcal{O}_i\}$ in these last two lines to proceed with a comparison with the l.h.s..

In the infinite- N_c limit, however, only the first term is non-vanishing because it is the only one that generates a factor of N_c in the trace. Thus, what remains to be shown for the statement about the decoupling of the flow equations is that

$$\text{STr}(\tilde{\partial}_t [P^{-1} \mathcal{O}_i P^{-1} \mathcal{O}_j]) \propto \delta_{ij}. \quad (\text{E3})$$

For the choice of $\mathcal{O}_i \in \{\mathbb{1}, \gamma^\mu, \gamma^{\text{ch}}\}$, this is indeed the

case. We split the free propagator into two parts,

$$P^{-1} = a_k \mathbb{1} + b_k p_\mu \gamma^\mu, \quad (\text{E4})$$

where the regulator derivative only acts on the scale-dependent coefficients a_k and b_k . We now separate the trace over Dirac space from the momentum integration. We immediately see that

$$\text{tr}(\mathbb{1} \mathcal{O}_i \mathbb{1} \mathcal{O}_j) \propto \delta_{ij}. \quad (\text{E5})$$

Moreover, linear parts in momentum vanish by integration if we evaluate at zero external momenta. Similarly, integration simplifies $p_\mu p_\nu \rightarrow \delta_{\mu\nu} p^2/d$ such that we only need to prove $\text{tr}(\gamma_\mu \mathcal{O}_i \gamma^\mu \mathcal{O}_j) \propto \delta_{ij}$.

- For $\mathcal{O}_i = \mathbb{1}$, this is clear using $\gamma_\mu \gamma^\mu = d$.
- For $\mathcal{O}_i = \gamma^{\text{ch}}$, it follows from the first point and that the trace over an odd number of gamma-matrices vanishes.
- For $\mathcal{O}_i = \gamma^\alpha$, we can even infer that

$$\text{tr}(\gamma_\mu \gamma^\alpha \gamma^\mu \gamma^\beta) \propto (2-d) \delta^{\alpha\beta} = 0, \quad (\text{E6})$$

which explains why there is no contribution to the flow of λ_3 in the infinite- N_c limit.

-
- [1] F. Gross *et al.*, 50 Years of Quantum Chromodynamics, *Eur. Phys. J. C* **83**, 1125 (2023), [arXiv:2212.11107 \[hep-ph\]](#).
- [2] V. Schön and M. Thies, 2-D model field theories at finite temperature and density, in *At The Frontier of Particle Physics: Handbook of QCD, Boris Ioffe Festschrift*, Vol. 3 (World Scientific, 2000) Chap. 33, pp. 1945–2032, [arXiv:hep-th/0008175](#).
- [3] E. Abdalla and M. C. B. Abdalla, Updating QCD in two-dimensions, *Phys. Rept.* **265**, 253 (1996), [arXiv:hep-th/9503002](#).
- [4] B. Andersson, *The Lund Model*, Cambridge Monographs on Particle Physics, Nuclear Physics and Cosmology, Vol. 7 (Cambridge University Press, 2023).
- [5] G. 't Hooft, A Two-Dimensional Model for Mesons, *Nucl. Phys. B* **75**, 461 (1974).
- [6] A. R. Zhitnitsky, On Chiral Symmetry Breaking in QCD in Two-dimensions ($N_c \rightarrow \text{Infinity}$), *Phys. Lett. B* **165**, 405 (1985).
- [7] G. 't Hooft, A planar diagram theory for strong interactions, *Nucl. Phys. B* **72**, 461 (1974).
- [8] W. R. Gutierrez, Path Integral Approach to the Large N Expansion of the Two-dimensional $u(n)$ QCD, *Nucl. Phys. B* **176**, 185 (1980).
- [9] S. J. Brodsky, H.-C. Pauli, and S. S. Pinsky, Quantum chromodynamics and other field theories on the light cone, *Phys. Rept.* **301**, 299 (1998), [arXiv:hep-ph/9705477](#).
- [10] P. D. Mannheim, P. Lowdon, and S. J. Brodsky, Comparing light-front quantization with instant-time quantization, *Phys. Rept.* **891**, 1 (2021), [arXiv:2005.00109 \[hep-ph\]](#).
- [11] F. Ambrosino and S. Komatsu, 2d QCD and Integrability, Part I: 't Hooft model (2023), [arXiv:2312.15598 \[hep-th\]](#).
- [12] F. Ambrosino and S. Komatsu, 2d QCD and Integrability, Part II: Generalized QCD (2024), [arXiv:2406.11078 \[hep-th\]](#).
- [13] A. Litvinov and P. Meshcheriakov, Meson mass spectrum in QCD₂ 't Hooft's model (2024), [arXiv:2409.11324 \[hep-th\]](#).
- [14] V. Schon and M. Thies, Decompactification of space or time in large N QCD(2), *Phys. Lett. B* **481**, 299 (2000), [arXiv:hep-th/0001162](#).
- [15] S. Cordes, G. W. Moore, and S. Ramgoolam, Lectures on 2-d Yang-Mills theory, equivariant cohomology and topological field theories, *Nucl. Phys. B Proc. Suppl.* **41**, 184 (1995), [arXiv:hep-th/9411210](#).
- [16] M. Blau and G. Thompson, Lectures on 2-d gauge theories: Topological aspects and path integral techniques, in *Summer School in High-energy Physics and Cosmology (Includes Workshop on Strings, Gravity, and*

- Related Topics 29-30 Jul 1993*) (1993) pp. 0175–244, [arXiv:hep-th/9310144](#).
- [17] A. A. Migdal, Recursion Equations in Gauge Theories, *Sov. Phys. JETP* **42**, 413 (1975).
- [18] E. Witten, On quantum gauge theories in two-dimensions, *Commun. Math. Phys.* **141**, 153 (1991).
- [19] E. Witten, Two-dimensional gauge theories revisited, *J. Geom. Phys.* **9**, 303 (1992), [arXiv:hep-th/9204083](#).
- [20] E. Abdalla, M. C. B. Abdalla, and K. D. Rothe, *Nonperturbative methods in 2 dimensional quantum field theory*, 2nd ed. (World Scientific, 2001).
- [21] R. M. Konik, M. Lajer, R. D. Pisarski, and A. M. Tsvelik, Nuclear Matter in 1 + 1 Dimensions, *Universe* **7**, 411 (2021), [arXiv:2202.01016 \[hep-ph\]](#).
- [22] M. Lajer, R. M. Konik, R. D. Pisarski, and A. M. Tsvelik, When cold, dense quarks in 1+1 and 3+1 dimensions are not a Fermi liquid, *Phys. Rev. D* **105**, 054035 (2022), [arXiv:2112.10238 \[hep-th\]](#).
- [23] G. Bergner, S. Piemonte, and M. Ünsal, Investigating two-dimensional adjoint QCD on the lattice, *JHEP* **7** (48), 48, [arXiv:2404.03801 \[hep-lat\]](#).
- [24] J. A. Damia, G. Galati, and L. Tizzano, Symmetries, Universes and Phases of QCD₂ with an Adjoint Dirac Fermion (2024), [arXiv:2409.17989 \[hep-th\]](#).
- [25] R. C. Farrell, I. A. Chernyshev, S. J. M. Powell, N. A. Zemlevskiy, M. Illa, and M. J. Savage, Preparations for quantum simulations of quantum chromodynamics in 1+1 dimensions. I. Axial gauge, *Phys. Rev. D* **107**, 054512 (2023), [arXiv:2207.01731 \[quant-ph\]](#).
- [26] R. C. Farrell, I. A. Chernyshev, S. J. M. Powell, N. A. Zemlevskiy, M. Illa, and M. J. Savage, Preparations for quantum simulations of quantum chromodynamics in 1+1 dimensions. II. Single-baryon β -decay in real time, *Phys. Rev. D* **107**, 054513 (2023), [arXiv:2209.10781 \[quant-ph\]](#).
- [27] H. Liu, T. Bhattacharya, S. Chandrasekharan, and R. Gupta, Phases of 2d massless QCD with qubit regularization (2023), [arXiv:2312.17734 \[hep-lat\]](#).
- [28] Y. Y. Atas, J. F. Haase, J. Zhang, V. Wei, S. M. L. Pfaendler, R. Lewis, and C. A. Muschik, Simulating one-dimensional quantum chromodynamics on a quantum computer: Real-time evolutions of tetra- and pentaquarks, *Phys. Rev. Res.* **5**, 033184 (2023), [arXiv:2207.03473 \[quant-ph\]](#).
- [29] A. N. Ciavarella, Quantum simulation of lattice QCD with improved Hamiltonians, *Phys. Rev. D* **108**, 094513 (2023), [arXiv:2307.05593 \[hep-lat\]](#).
- [30] E. Oevermann, *Renormalization group flow of QCD in 1+1 Dimensions*, *Master thesis*, Friedrich-Schiller-Universität Jena, Jena (2024).
- [31] Y. Frishman and J. Sonnenschein, Non-Perturbative Field Theory – From Two Dimensional Conformal field Theory to QCD in Four Dimensions (2010), [arXiv:1004.4859 \[hep-th\]](#).
- [32] M. Shifman, *Advanced topics in quantum field theory: A lecture course* (Cambridge Univ. Press, Cambridge, UK, 2012).
- [33] S. R. Coleman, *Aspects of Symmetry: Selected Erice Lectures* (Cambridge University Press, Cambridge, U.K., 1985).
- [34] N. D. Mermin and H. Wagner, Absence of ferromagnetism or antiferromagnetism in one- or two-dimensional isotropic Heisenberg models, *Phys. Rev. Lett.* **17**, 1133 (1966).
- [35] S. R. Coleman, There are no Goldstone bosons in two-dimensions, *Commun. Math. Phys.* **31**, 259 (1973).
- [36] P. C. Hohenberg, Existence of long-range order in one and two dimensions, *Phys. Rev.* **158**, 383 (1967).
- [37] V. L. Berezinskii, Destruction of Long-range Order in One-dimensional and Two-dimensional Systems having a Continuous Symmetry Group I. Classical Systems, *Sov. Phys. JETP* **32**, 493 (1971).
- [38] V. L. Berezinsky, Destruction of Long-range Order in One-dimensional and Two-dimensional Systems Possessing a Continuous Symmetry Group. II. Quantum Systems., *Sov. Phys. JETP* **34**, 610 (1972).
- [39] J. M. Kosterlitz and D. J. Thouless, Ordering, metastability and phase transitions in two-dimensional systems, *J. Phys. C* **6**, 1181 (1973).
- [40] B. S. DeWitt, *Dynamical theory of groups and fields* (Gordon and Breach, New York, USA, 1965).
- [41] R. E. Kallosh, The Renormalization in Nonabelian Gauge Theories, *Nucl. Phys. B* **78**, 293 (1974).
- [42] J. Honerkamp, The Question of invariant renormalizability of the massless Yang-Mills theory in a manifest covariant approach, *Nucl. Phys. B* **48**, 269 (1972).
- [43] I. Y. Arefeva, L. D. Faddeev, and A. A. Slavnov, Generating Functional for the s Matrix in Gauge Theories, *Teor. Mat. Fiz.* **21**, 311 (1974).
- [44] S. Sarkar, Mixing of Operators in Wilson Expansions, *Nucl. Phys. B* **82**, 447 (1974).
- [45] S. Sarkar and H. Strubbe, Anomalous Dimensions in Background Field Gauges, *Nucl. Phys. B* **90**, 45 (1975).
- [46] H. Kluberg-Stern and J.-B. Zuber, Renormalization of Nonabelian Gauge Theories in a Background Field Gauge. 1. Green Functions, *Phys. Rev. D* **12**, 482 (1975).
- [47] H. Kluberg-Stern and J.-B. Zuber, Renormalization of Nonabelian Gauge Theories in a Background Field Gauge. 2. Gauge Invariant Operators, *Phys. Rev. D* **12**, 3159 (1975).
- [48] G. 't Hooft, An algorithm for the poles at dimension four in the dimensional regularization procedure, *Nucl. Phys. B* **62**, 444 (1973).
- [49] M. T. Grisaru, P. van Nieuwenhuizen, and C. C. Wu, Background Field Method Versus Normal Field Theory in Explicit Examples: One Loop Divergences in S Matrix and Green's Functions for Yang-Mills and Gravitational Fields, *Phys. Rev. D* **12**, 3203 (1975).
- [50] L. F. Abbott, The Background Field Method Beyond One Loop, *Nucl. Phys. B* **185**, 189 (1981).
- [51] L. F. Abbott, Introduction to the Background Field Method, *Acta Phys. Polon. B* **13**, 33 (1982).
- [52] M. E. Peskin and D. V. Schroeder, *An introduction to quantum field theory* (Addison-Wesley, Reading, USA, 1995).
- [53] N. Dupuis, L. Canet, A. Eichhorn, W. Metzner, J. M. Pawłowski, M. Tissier, and N. Wschebor, The nonperturbative functional renormalization group and its applications, *Phys. Rept.* **910**, 1 (2021), [arXiv:2006.04853 \[cond-mat.stat-mech\]](#).
- [54] L. D. Faddeev and V. N. Popov, Feynman Diagrams for the Yang-Mills Field, *Phys. Lett. B* **25**, 29 (1967).
- [55] V. N. Gribov, Quantization of Nonabelian Gauge Theories, *Nucl. Phys. B* **139**, 1 (1978).
- [56] N. Vandersickel and D. Zwanziger, The Gribov problem and QCD dynamics, *Phys. Rept.* **520**, 175 (2012),

- arXiv:1202.1491 [hep-th].
- [57] D. H. Dudal, S. P. Sorella, N. Vandersickel, and H. Verschelde, The Effects of Gribov copies in 2D gauge theories, *Phys. Lett. B* **680**, 377 (2009), arXiv:0808.3379 [hep-th].
- [58] F. Freire, D. F. Litim, and J. M. Pawłowski, Gauge invariance and background field formalism in the exact renormalization group, *Phys. Lett. B* **495**, 256 (2000), arXiv:hep-th/0009110.
- [59] H. Gies, Introduction to the Functional RG and applications to gauge theories, *Lect. Notes Phys.* **852**, 287 (2012), arXiv:hep-ph/0611146.
- [60] C. Becchi, A. Rouet, and R. F. Stora, Renormalization of Gauge Theories, *Annals Phys.* **98**, 287 (1976).
- [61] I. V. Tyutin, Gauge Invariance in Field Theory and Statistical Physics in Operator Formalism (1975), arXiv:0812.0580 [hep-th].
- [62] K. Osterwalder and R. Schrader, Axioms for Euclidean Green's Functions, *Commun. Math. Phys.* **31**, 83 (1973).
- [63] K. Osterwalder and R. Schrader, Axioms for Euclidean Green's Functions. 2., *Commun. Math. Phys.* **42**, 281 (1975).
- [64] J. Braun, Y.-r. Chen, W.-j. Fu, A. Geißel, J. Horak, C. Huang, F. Ihssen, J. M. Pawłowski, M. Reichert, F. Rennecke, Y.-y. Tan, S. Töpfel, J. Wessely, and N. Wink, Renormalised spectral flows, *SciPost Phys. Core* **6**, 061 (2023), arXiv:2206.10232 [hep-th].
- [65] R. Gurau, V. Rivasseau, and A. Sfondrini, Renormalization: an advanced overview (2014), arXiv:1401.5003 [hep-th].
- [66] C. Wetterich, Exact evolution equation for the effective potential, *Phys. Lett. B* **301**, 90 (1993), arXiv:1710.05815 [hep-th].
- [67] T. R. Morris, The Exact Renormalization Group and approximate solutions, *Int. J. Mod. Phys. A* **09**, 2411 (1994), arXiv:hep-ph/9308265.
- [68] U. Ellwanger, Flow equations for N point functions and bound states, *Z. Phys. C* **62**, 503 (1994), arXiv:hep-ph/9308260.
- [69] A. Koenigstein, *Non-perturbative aspects of (low-dimensional) quantum field theories*, Phd thesis, Universitätsbibliothek Johann Christian Senckenberg (2023).
- [70] J. M. Pawłowski, Aspects of the functional renormalisation group, *Annals Phys.* **322**, 2831 (2007), arXiv:hep-th/0512261.
- [71] F. Rennecke, *The chiral phase transition of QCD*, Phd thesis, University of Heidelberg (2015).
- [72] P. Kopietz, L. Bartosch, and F. Schütz, *Introduction to the Functional Renormalization Group*, Lecture Notes in Physics, Vol. 798 (Springer-Verlag Berlin Heidelberg, 2010).
- [73] J. Berges, N. Tetradis, and C. Wetterich, Nonperturbative renormalization flow in quantum field theory and statistical physics, *Phys. Rept.* **363**, 223 (2002), arXiv:hep-ph/0005122.
- [74] D. F. Litim, Optimization of the exact renormalization group, *Phys. Lett. B* **486**, 92 (2000), arXiv:hep-th/0005245.
- [75] D. F. Litim, Optimized renormalization group flows, *Phys. Rev. D* **64**, 105007 (2001), arXiv:hep-th/0103195.
- [76] L. Canet, B. Delamotte, D. Mouhanna, and J. Vidal, Optimization of the derivative expansion in the non-perturbative Renormalization Group, *Phys. Rev. D* **67**, 065004 (2003), arXiv:hep-th/0211055.
- [77] L. Canet, B. Delamotte, D. Mouhanna, and J. Vidal, Nonperturbative Renormalization Group approach to the Ising model: A derivative expansion at order ∂^4 , *Phys. Rev. B* **68**, 064421 (2003), arXiv:hep-th/0302227.
- [78] O. J. Rosten, Fundamentals of the Exact Renormalization Group, *Phys. Rept.* **511**, 177 (2012), arXiv:1003.1366 [hep-th].
- [79] H. Osborn and D. E. Twigg, Remarks on Exact RG equations, *Annals Phys.* **327**, 29 (2012), arXiv:1108.5340 [hep-th].
- [80] J. M. Pawłowski, M. M. Scherer, R. Schmidt, and S. J. Wetzel, Physics and the choice of regulators in functional renormalisation group flows, *Annals Phys.* **384**, 165 (2017), arXiv:1512.03598 [hep-th].
- [81] I. Balog, H. Chaté, B. Delamotte, M. Marohnic, and N. Wschebor, Convergence of nonperturbative approximations to the Renormalization Group, *Phys. Rev. Lett.* **123**, 240604 (2019), arXiv:1907.01829 [cond-mat.stat-mech].
- [82] J. Braun, T. Dörfel, B. Schallmo, and S. Töpfel, Renormalization group studies of dense relativistic systems, *Phys. Rev. D* **104**, 096002 (2021), arXiv:2008.05978 [hep-ph].
- [83] N. Zorbach, J. Stoll, and J. Braun, Optimization and Stabilization of Functional Renormalization Group Flows (2024), arXiv:2401.12854 [hep-ph].
- [84] D.-U. Jungnickel and C. Wetterich, Effective action for the chiral quark-meson model, *Phys. Rev. D* **53**, 5142 (1996), arXiv:hep-ph/9505267.
- [85] H. Gies and C. Wetterich, Universality of spontaneous chiral symmetry breaking in gauge theories, *Phys. Rev. D* **69**, 025001 (2004), arXiv:hep-th/0209183.
- [86] H. Gies and J. Jaeckel, Chiral phase structure of QCD with many flavors, *Eur. Phys. J. C* **46**, 433 (2006), arXiv:hep-ph/0507171.
- [87] W. E. Thirring, A soluble relativistic field theory, *Annals Phys.* **3**, 91 (1958).
- [88] D. J. Gross and A. Neveu, Dynamical Symmetry Breaking in Asymptotically Free Field Theories, *Phys. Rev. D* **10**, 3235 (1974).
- [89] R. F. Dashen, B. Hasslacher, and A. Neveu, Semiclassical Bound States in an Asymptotically Free Theory, *Phys. Rev. D* **12**, 2443 (1975).
- [90] J. J. Lenz, L. Pannullo, M. Wagner, B. H. Welleghausen, and A. Wipf, Baryons in the Gross-Neveu model in 1+1 dimensions at finite number of flavors, *Phys. Rev. D* **102**, 114501 (2020), arXiv:2007.08382 [hep-lat].
- [91] U. Wolff, The phase diagram of the infinite-N Gross-Neveu model at finite temperature and chemical potential, *Phys. Lett. B* **157**, 303 (1985).
- [92] O. Schnetz, M. Thies, and K. Urlichs, Phase diagram of the Gross-Neveu model: Exact results and condensed matter precursors, *Annals Phys.* **314**, 425 (2004), arXiv:hep-th/0402014.
- [93] G. Basar, G. V. Dunne, and M. Thies, Inhomogeneous condensates in the thermodynamics of the chiral NJL₂ model, *Phys. Rev. D* **79**, 105012 (2009), arXiv:0903.1868 [hep-th].
- [94] Y. Nambu and G. Jona-Lasinio, Dynamical model of elementary particles based on an analogy with superconductivity. II, *Phys. Rev.* **124**, 246 (1961).
- [95] Y. Nambu and G. Jona-Lasinio, Dynamical model of elementary particles based on an analogy with super-

- conductivity. I, *Phys. Rev.* **122**, 345 (1961).
- [96] J. Braun, M. Leonhardt, and M. Pospiech, Fierz-complete NJL model study: Fixed points and phase structure at finite temperature and density, *Phys. Rev. D* **96**, 076003 (2017), arXiv:1705.00074 [hep-ph].
- [97] J. Braun, M. Leonhardt, and M. Pospiech, Fierz-complete NJL model study. II. Toward the fixed-point and phase structure of hot and dense two-flavor QCD, *Phys. Rev. D* **97**, 076010 (2018), arXiv:1801.08338 [hep-ph].
- [98] J. Braun, M. Leonhardt, and M. Pospiech, Fierz-complete NJL model study III: Emergence from quark-gluon dynamics, *Phys. Rev. D* **101**, 036004 (2020), arXiv:1909.06298 [hep-ph].
- [99] K.-I. Aoki, K. Morikawa, J.-I. Sumi, H. Terao, and M. Tomoyose, Wilson renormalization group equations for the critical dynamics of chiral symmetry, *Prog. Theor. Phys.* **102**, 1151 (1999), arXiv:hep-th/9908042.
- [100] J. Braun, Fermion Interactions and Universal Behavior in Strongly Interacting Theories, *J. Phys. G* **39**, 033001 (2012), arXiv:1108.4449 [hep-ph].
- [101] K.-I. Aoki and M. Yamada, The RG flow of Nambu–Jona-Lasinio model at finite temperature and density, *Int. J. Mod. Phys. A* **30**, 1550180 (2015), arXiv:1504.00749 [hep-ph].
- [102] W.-j. Fu, C. Huang, J. M. Pawłowski, and Y.-y. Tan, Four-quark scatterings in QCD I, *SciPost Phys.* **14**, 069 (2023), arXiv:2209.13120 [hep-ph].
- [103] W.-j. Fu, C. Huang, J. M. Pawłowski, and Y.-y. Tan, Four-quark scatterings in QCD II (2024), arXiv:2401.07638 [hep-ph].
- [104] F. Ihssen, J. M. Pawłowski, F. R. Sattler, and N. Wink, Towards quantitative precision for QCD at large densities (2023), arXiv:2309.07335 [hep-th].
- [105] J. O. Andersen, W. R. Naylor, and A. Tranberg, Phase diagram of QCD in a magnetic field: A review, *Rev. Mod. Phys.* **88**, 025001 (2016), arXiv:1411.7176 [hep-ph].
- [106] M. Buballa, NJL model analysis of quark matter at large density, *Phys. Rept.* **407**, 205 (2005), arXiv:hep-ph/0402234.
- [107] P. Springer, J. Braun, S. Rechenberger, and F. Rennecke, QCD-inspired determination of NJL model parameters, *EPJ Web Conf.* **137**, 03022 (2017), arXiv:1611.06020 [hep-ph].
- [108] M. Thies, Chiral spiral in the presence of chiral imbalance, *Phys. Rev. D* **98**, 096019 (2018), arXiv:1810.03921 [hep-th].
- [109] M. Thies, Duality study of the chiral Heisenberg-Gross-Neveu model in 1+1 dimensions, *Phys. Rev. D* **102**, 096006 (2020), arXiv:2008.13119 [hep-th].
- [110] M. Thies and K. Ulrichs, Revised phase diagram of the Gross-Neveu model, *Phys. Rev. D* **67**, 125015 (2003), arXiv:hep-th/0302092.
- [111] M. Q. Huber, A. K. Cyrol, and J. M. Pawłowski, DoFun 3.0: Functional equations in Mathematica, *Comput. Phys. Commun.* **248**, 107058 (2020), arXiv:1908.02760 [hep-ph].
- [112] Wolfram Research, Inc., *Mathematica, Version 13.0* (2023).
- [113] A. K. Cyrol, M. Mitter, and N. Strodthoff, FormTracer - A Mathematica Tracing Package Using FORM, *Comput. Phys. Commun.* **219**, 346 (2017), arXiv:1610.09331 [hep-ph].
- [114] H. Gies, Running coupling in Yang-Mills theory: A flow equation study, *Phys. Rev. D* **66**, 025006 (2002), arXiv:hep-th/0202207.
- [115] J. Hubbard, Calculation of partition functions, *Phys. Rev. Lett.* **3**, 77 (1959).
- [116] R. L. Stratonovich, On a Method of Calculating Quantum Distribution Functions, *Sov. Phys. Dokl.* **2**, 416 (1957).
- [117] W. Metzner, M. Salmhofer, C. Honerkamp, V. Meden, and K. Schonhammer, Functional renormalization group approach to correlated fermion systems, *Rev. Mod. Phys.* **84**, 299 (2012), arXiv:1105.5289 [cond-mat.str-el].
- [118] M. Thies, From relativistic quantum fields to condensed matter and back again: Updating the Gross-Neveu phase diagram, *J. Phys. A* **39**, 12707 (2006), arXiv:hep-th/0601049.
- [119] C. Boehmer and M. Thies, Large N solution of generalized Gross-Neveu model with two coupling constants, *Phys. Rev. D* **80**, 125038 (2009), arXiv:0909.3714 [hep-th].
- [120] M. Thies, Phase structure of the (1 + 1)-dimensional Nambu-Jona-Lasinio model with isospin, *Phys. Rev. D* **101**, 014010 (2020), arXiv:1911.11439 [hep-th].
- [121] H. Gies and C. Wetterich, Renormalization flow of bound states, *Phys. Rev. D* **65**, 065001 (2002), arXiv:hep-th/0107221.
- [122] S. Floerchinger and C. Wetterich, Exact flow equation for composite operators, *Phys. Lett. B* **680**, 371 (2009), arXiv:0905.0915 [hep-th].
- [123] F. Ihssen and J. M. Pawłowski, Physics-informed renormalisation group flows (2024), arXiv:2409.13679 [hep-th].
- [124] D. Gkiatas, *Towards a BRST-invariant construction of pure Yang-Mills theory*, Ph.D. thesis, University Jena (2023).
- [125] N. Nakanishi, Covariant Quantization of the Electromagnetic Field in the Landau Gauge, *Prog. Theor. Phys.* **35**, 1111 (1966).
- [126] B. E. Lautrup, Canonical quantum electrodynamics in covariant gauges, *K. Dan. Vidensk. Selsk. Mat. Fys. Medd.* **35** (1967).